THE JOURNAL OF BIOLOGICAL CHEMISTRY
Vol. 279, No. 48, Issue of November 26, pp. 50482–50498, 2004
Printed in U.S.A.

The Aldehyde Oxidase Gene Cluster in Mice and Rats

ALDEHYDE OXIDASE HOMOLOGUE 3, A NOVEL MEMBER OF THE MOLYBDO-FLAVOENZYME FAMILY WITH SELECTIVE EXPRESSION IN THE OLFACTORY MUCOSA*

Received for publication, August 2, 2004, and in revised form, September 20, 2004
Published, JBC Papers in Press, September 20, 2004, DOI 10.1074/jbc.M408734200

Mami Kurosaki‡§, Mineko Terao‡§, Maria Monica Barzago‡, Antonio Bastone¶, Davide Bernardinello¶, Mario Salmona¶, and Enrico Garattini‡‖

From the ‡Laboratory of Molecular Biology, Centro Catullo e Daniela Borgomainerio, and the ¶Department of Biochemistry and Molecular Pharmacology, Istituto di Ricerche Farmacologiche "Mario Negri," via Eritrea 62, 20157 Milan, Italy

Mammalian molybdo-flavoenzymes are oxidases requiring FAD and molybdopterin (molybdenum cofactor) for their catalytic activity. This family of proteins was thought to consist of four members, xanthine oxidoreductase, aldehyde oxidase 1 (AOX1), and the aldehyde oxidase homologues 1 and 2 (AOH1 and AOH2, respectively). Whereas the first two enzymes are present in humans and various other mammalian species, the last two proteins have been described only in mice. Here, we report on the identification, in both mice and rats, of a novel molybdo-flavoenzyme, AOH3. In addition, we have cloned the cDNAs coding for rat AOH1 and AOH2, demonstrating that this animal species has the same complement of molybdo-flavoproteins as the mouse. The AOH3 cDNA is characterized by remarkable similarity to AOX1, AOH1, AOH2, and xanthine oxidoreductase cDNAs. Mouse AOH3 is selectively expressed in Bowman's glands of the olfactory mucosa, although small amounts of the corresponding mRNA are present also in the skin. In the former location, two alternatively spliced forms of the AOH3 transcript with different 3′-untranslated regions were identified. The general properties of AOH3 were determined by purification of mouse AOH3 from the olfactory mucosa. The enzyme possesses aldehyde oxidase activity and oxidizes, albeit with low efficiency, exogenous substrates that are recognized by AOH1 and AOX1. The *Aoh3* gene maps to mouse chromosome 1 band c1 and rat chromosome 7 in close proximity to the *Aox1*, *Aoh1*, and *Aoh2* loci and has an exon/intron structure almost identical to that of the other molybdo-flavoenzyme genes in the two species.

Molybdo-flavoenzymes are a subgroup of molybdo-proteins requiring molybdopterin (molybdenum cofactor) and a flavin cofactor for their catalytic activity (1–3). These proteins are present throughout evolution from bacteria to man (1, 4–6). In mammals, four distinct molybdo-flavoenzymes have been identified: xanthine oxidoreductase (XOR)[1] (7–11), aldehyde oxidase 1 (AOX1) (12, 13), and aldehyde oxidase homologues 1 and 2 (AOH1 and AOH2, respectively) (14, 15). Whereas XOR and AOX1 have been isolated and characterized in humans (8, 12, 16), rodents (17–19), and bovines (13, 20, 21), AOH1 and AOH2 have been identified only in mice (14, 15). Mammalian molybdo-flavoenzymes are cytosolic proteins consisting of dimers of two identical subunits (1). The amino acid sequence of the ~150-kDa subunit of all members of the family is highly conserved, suggesting a related evolutionary origin from a common ancestor protein (1). XOR, AOX1, AOH1, and AOH2 are the products of distinct genes that maintain an almost superimposing structural organization (15). This suggests that the extant members of the mammalian molybdo-flavoenzyme family arose from one or more gene duplication events (1). In mice, *Xor* maps to chromosome 17 (18), whereas *Aox1*, *Aoh1*, and *Aoh2* constitute an aldehyde oxidase gene cluster on chromosome 1 band c1 (15).

XOR is a relatively ubiquitous enzyme, being present in many tissues and cell types, although it is synthesized in high amounts in the intestinal tract, liver, and lactating mammary gland (22). XOR catalyzes the oxidation of hypoxanthine to xanthine and xanthine to uric acid (23), representing a key enzyme in the catabolism of purines (22, 23). However, the protein may have other tissue- or cell-specific functions, as suggested by the phenotype observed in the *Xor* knockout mouse (24). Much less is known about the physiological role and substrates of the other members of the family. AOX1 and AOH1 are predominantly expressed in the liver and lung and metabolize retinaldehyde into retinoic acid (14, 15, 17, 25–27), which is the active metabolite of vitamin A, a known morphogen (28, 29) and a key regulator of many tissues and cell types in the adult animal. Thus, AOX1 and AOH1 may be of relevance to the development of vertebrates and may control the homeostasis of certain types of tissues in adults. Virtually nothing is known about the substrate specificity of AOH2. In fact, the enzyme is difficult to purify, as it is present in relatively low quantities only in keratinized epithelia (14, 15). AOX1 is an enzyme of pharmacological and toxicological importance. In fact, this aldehyde oxidase metabolizes numerous xenobiotics, including drugs such as zaleplon (30) and 6-mer-

* This work was supported by grants from the Fondo Italiano Ricerca Biotecnologica, the Consiglio Nazionale delle Ricerche (Progetto Finalizzato Biotecnologie), the Fondazione Italo Monzino, and the Associazione Italiana per la Ricerca Contro il Cancro. The costs of publication of this article were defrayed in part by the payment of page charges. This article must therefore be hereby marked "*advertisement*" in accordance with 18 U.S.C. Section 1734 solely to indicate this fact.

The nucleotide sequence(s) reported in this paper has been submitted to the GenBank™/EBI Data Bank with accession number(s) AY665586, AY665587, AY665588, AY665589, and AY187018.

§ Both authors contributed equally to this work.

‖ To whom correspondence should be addressed. Tel.: 39-2-3901-4533; Fax: 39-2-354-6277; E-mail: egarattini@marionegri.it.

[1] The abbreviations used are: XOR, xanthine oxidoreductase; AOX1, aldehyde oxidase 1; AOH1, AOH2, and AOH3, aldehyde oxidase homologues 1–3, respectively; RT, reverse transcription; RACE, rapid amplification of cDNA ends; MALDI-TOF, matrix-assisted laser desorption ionization time-of-flight; EST, expressed sequence tag; 3′-UTR, 3′-untranslated region.

captopurine (31) and pollutants such as nitropolycyclic hydrocarbons (32). The enzyme has also been implicated in the hepatotoxicity of ethanol in humans and other mammals, as AOX1 oxidizes the toxic metabolite acetaldehyde into acetic acid (33). We proposed that AOH1 may play a similar role in the mouse; however, studies conducted on purified mouse AOX1 and AOH1 indicate that acetaldehyde is a relatively poor substrate for the two enzymes (34). In addition, results obtained in mouse strains characterized by the synthesis of remarkably different levels of both AOH1 and AOX1 show the same level of acetaldehyde metabolism *in vivo* (34).

In this study, we demonstrate that the family of mammalian molybdo-flavoenzymes is larger than originally believed. In fact, we have identified and isolated mouse AOH3, a novel molybdo-flavoenzyme characterized by high similarity to AOX1, AOH1, AOH2, and, to a lesser extent, XOR. The protein is endowed with aldehyde oxidase activity and is selectively expressed in the epithelial mucosa at the level of Bowman's glands. The corresponding cDNAs have been cloned and sequenced in both the mouse and rat. Isolation of the mouse and rat AOH3 cDNAs proved instrumental in the definition of the exon/intron structure of the corresponding genes, which are located on chromosomes 1 and 9, respectively. Finally, we have also cloned and sequenced the cDNAs of the mouse AOH1 and AOH2 orthologous proteins in rats, demonstrating that the two molybdo-enzymes are coded for by genes that cluster with *Aox1* and *Aoh3* on chromosome 9. These last results demonstrate that the presence of multiple forms of aldehyde oxidases in mammals is not a peculiarity of the mouse.

EXPERIMENTAL PROCEDURES

Cloning and Sequencing of cDNAs Coding for Mouse AOH3 and Rat AOH1, AOH2, and AOH3—Total RNA was extracted from mouse olfactory mucosa, and the poly(A^+) fraction of the RNA was selected according to standard protocols (14, 15). The full-length mouse AOH3 cDNA expressed in olfactory mucosa was isolated as two overlapping fragments, A (nucleotides 72–2332) and B (nucleotides 2247–4425), by reverse transcription followed by nested PCR amplifications. The oligonucleotides used for these experiments were as follows: primary amplimers, 5′-ATCCGAGCCAAGAGGCCAAACTCA-3′ (nucleotides 62–85) and 5′-CCTTTCCTTTCCCTCCATCTGCAGCA-3′ (complementary to nucleotides 4410–4435); and nested primers, 5′-AGAGGCCAAACTCACCAGAGCC-3′ (nucleotides 72–93), 5′-CTTCAGCTACCTGATCCACGTTCT-3′ (complementary to nucleotides 2309–2332), 5′-GCACAATTCGTTCCTGTGCCCTGAA-3′ (nucleotides 2247–2271), and 5′-CCCTCCATCTGCAGCAACATTTAC-3′ (complementary to nucleotides 4402–4425). The amplified DNA fragments (pAOH3-A and pAOH3-B) were subcloned into pBluescript (Stratagene, La Jolla, CA) with the AT cloning kit (Invitrogen) and sequenced. The mouse AOH3 cDNA was also isolated from skin poly(A^+) RNA in a similar way, and its nucleotide sequence was determined. Rat AOH1, AOH2, and AOH3 cDNAs were isolated from liver, skin, and olfactory mucosa poly(A^+) RNAs, respectively, by reverse transcription (RT)-PCR techniques using sense strand amplimers coding for the first eight N-terminal amino acids and antisense amplimers corresponding to the seven C-terminal amino acids and the stop codon. The resulting amplified cDNA fragments representing the entire coding regions of each protein were subcloned in pBluescript and sequenced.

Determination of the 5′- and 3′-Ends of the Mouse AOH3 Transcripts—The 5′- and 3′-rapid amplification of cDNA ends (RACE) experiments for the mouse AOH3 cDNAs were performed with the commercially available Marathon cDNA amplification kit (Clontech, Palo Alto, CA) according to the nested PCR protocol and using the following amplimers: SP1, 5′-CGGATCGTGTTGTGACACCATCACTG-3′ (complementary to nucleotides 263–288 of the mouse AOH3 cDNA); and NP1, 5′-TGTGACACCATCACTGTGCAGGC-3′ (complementary to nucleotides 256–278 of the mouse AOH3 cDNA). 3′-RACE of the mouse AOH3 cDNAs was conducted as described above with the following amplimers: SP2, 5′-AAGAGACATAGCGGAGGACTTCACAG-3′ (nucleotides 3990–4015); and NP2, 5′-GACTTCACAGTGAAGAGCCCAGCA-3′ (nucleotides 4006–4029). The resulting PCR products were subcloned in pBluescript, and multiple clones were sequenced to determine the 5′- and 3′-ends of the mouse AOH3 transcript.

In Situ Hybridization Experiments—The plasmid pAOH3-A was linearized with HindIII and used as template for the synthesis of antisense riboprobe employing T7 RNA polymerase (Stratagene) in the presence of [^{35}S]thio-UTP as described (14). Mouse tissues were fixed in 4% (w/v) paraformaldehyde overnight, embedded in paraffin, sectioned to 5-μm thickness, and mounted on gelatin-coated slides. The conditions for the pretreatment of slides, hybridization, washing, and detection by the nuclear track emulsion technique were as described in a previous report (14). At the end of the *in situ* hybridization procedure, tissue sections were stained with hematoxylin/eosin and photographed under a microscope.

Purification of Mouse Olfactory Mucosa AOH3 Protein, Electrophoresis, and Western Blot Analysis—Unless otherwise stated, all purification steps were carried out at 4 °C. Male mouse olfactory mucosa was dissected and homogenized in 3 volumes of 100 mM sodium phosphate buffer (pH 7.5) containing 0.1% Triton X-100 with an Ultraturrax homogenizer (Ika, Stanten, Germany). Homogenates were centrifuged at 100,000 × *g* for 45 min to obtain cytosolic extracts. Extracts were heated at 55 °C for 10 min and centrifuged at 15,000 × *g* to remove precipitated proteins. An equal volume of saturated ammonium sulfate was added to the supernatant, and the precipitate was collected by centrifugation at 100,000 × *g* and resuspended in 50 mM Tris-HCl (pH 7.5). The solution was passed through a Sephadex PD-10 column (Amersham Biosciences AB, Uppsala, Sweden) to eliminate the residual ammonium sulfate. The eluate (3.5 ml) was applied to a Mono Q 5/5 fast protein liquid chromatography column (Amersham Biosciences AB) equilibrated in 50 mM Tris-HCl (pH 7.4). The AOH3 protein was eluted at 0.5 ml/min with a linear gradient (30 ml) of 0–1 M NaCl in 50 mM Tris-HCl (pH 7.5). The purification of AOH3 was monitored by quantitative Western blot analysis (34).

A specific rabbit anti-AOH3 polyclonal antibody raised against a synthetic peptide of the protein (SGRIKALDIE, amino acids 868–877) was used for Western blot analysis, which was carried out following a chemiluminescence-based protocol as described (14, 15, 34). This antibody is monospecific and does not cross-react with purified mouse AOX1 and AOH1 and recombinant mouse XOR, AOX1, AOH1, and AOH2 transiently expressed in human epithelial kidney HEK293 cells (data not shown). For quantitative Western blot analysis, an equivalent volume (10 μl) of protein solution, at each purification step, was loaded on the same gel and processed for analysis. Chemiluminescent signals corresponding to AOH3 bands were quantitated with a scanning densitometer (Hoefer Scientific Instruments, San Francisco, CA). The total amount of AOH3 immunoreactive protein in the various experimental samples is expressed in arbitrary units and was calculated on the basis of the intensity of the Western blot signal in absorbance multiplied by the total volume of each purification step. One arbitrary unit of immunoreactive protein corresponds to 1.0 *A* unit of the specific AOH3 band in each experimental sample.

Zymographic analysis of aldehyde-oxidizing activity was performed following electrophoresis on cellulose acetate plates. Plates were overlaid with 1.2% agarose containing 0.3 mM phenazine methosulfate (Sigma), 0.9 mM 3-(4,5-dimethylthiazol-2-yl)-2,5-diphenyltetrazolium bromide (Sigma), and the selected enzyme substrate at 10 mM (14, 34). SDS-PAGE was performed according to standard techniques (14, 15, 34). Proteins were measured according to the Bradford method with a commercially available kit (Bio-Rad).

Characterization of the Purified AOH3 Protein by Mass Spectrometry—Matrix-assisted laser desorption ionization (MALDI) mass spectrometric and electrospray ionization tandem mass spectrometric analyses of AOH3 tryptic peptides were performed according to standard protocols following in-gel tryptic digestion (34). Briefly, the Coomassie Blue-stained gel slice corresponding to purified AOH3 was incubated with 10 mM dithiothreitol in 100 mM ammonium bicarbonate at 56 °C for 30 min to reduce disulfide bridges. Thiol groups were alkylated upon reaction with 55 mM iodoacetamide in 100 mM ammonium bicarbonate at room temperature in the dark for 20 min. Tryptic digestion was carried out overnight at 37 °C in 50 mM ammonium bicarbonate and 12.5 ng/μl trypsin (Promega, Madison, WI). Peptides were extracted twice in 50% acetonitrile and 5% formic acid. The combined extracts were lyophilized, redissolved in 0.5% formic acid, and desalted using ZipTip (Millipore Corp.). Peptides were eluted in 50% acetonitrile and 0.5% formic acid. The eluate was mixed 1:1 (v/v) with a saturated matrix solution of α-cyano-4-hydroxycinnamic acid in acetonitrile and 0.1% trifluoroacetic acid (1:3, v/v). Mass mapping of tryptic peptides was performed with a Bruker Reflex III MALDI-TOF mass spectrometer. The data generated were processed with the Mascot program (www.matrixscience.com/) (34), allowing a mass tolerance of ≤0.1 Da. *De novo* sequence analysis was carried out via collision-induced dissociation on

an API 3000 electrospray mass spectrometer (Applied Biosystems, San Diego, CA). The data were confirmed by comparison of the experimental and theoretical collision-induced dissociation spectra of the tryptic peptides derived from the AOH3 protein sequence derived from the corresponding cDNA.

DNA Sequencing and Determination of the Exon/Intron Structure of the Mouse Aoh3 and Rat Aoh1, Aoh2, and Aoh3 Genes—Appropriate DNA fragments were subcloned into the pBluescript plasmid vector and sequenced according to the Sanger dideoxy chain termination method using double-stranded DNA as template and T7 DNA polymerase (Amersham Biosciences AB) or Sequenase (U. S. Biochemical Corp.). Oligodeoxynucleotide primers were custom-synthesized by M-Medical srl (Florence, Italy). Computer analysis of the DNA sequences was performed using the GeneWorks sequence analysis system (Intelligenetics, San Diego). Comparison of the nucleotide and protein sequences of the full-length cDNAs corresponding to mouse AOH3 and rat AOH1, AOH2, and AOH3 with the complete mouse and rat genomic sequences present in the NCBI Database resulted in the determination of the exon/intron structure of the corresponding genes.

RESULTS

Cloning and Characterization of the Mouse cDNA Coding for the Novel Molybdo-flavoprotein AOH3—In silico analysis of the NCBI Database for nucleotide sequences of the mouse genome showing similarity to the AOX1, AOH1, and AOH2 cDNAs resulted in the identification of exons coding for a potential and novel molybdo-flavoprotein, which we named AOH3. The identified exon sequences were used for the design of appropriate oligonucleotides that allowed the amplification of overlapping cDNA fragments of mouse AOH3 by RT-PCR from olfactory mucosa and, subsequently, from skin RNA. The first source of AOH3 RNA was selected on the basis of a preliminary search in the mouse expressed sequence tag (EST) data base.

Fig. 1 illustrates the nucleotide sequence of the full-length AOH3 cDNA isolated from mouse olfactory mucosa. The 5′-untranslated region is relatively short (93 nucleotides) and contains a stretch of DNA around the putative first methionine codon (GCCATGC) that is similar to the canonical ribosome-binding consensus sequence (RCCATGG) (35). The 3′-untranslated region is much longer and is characterized by the absence of a canonical polyadenylation signal. As this portion of the cDNA was obtained by 3′-RACE, the lack of a polyadenylation signal is likely to be the result of the synthesis of an incomplete 3′ terminus. In fact, a typical polyadenylation consensus sequence (AATAAA) is present in the mouse genome (NCBI accession no. NT_039170), 215 bases downstream of the nucleotide corresponding to the last base of our AOH3 cDNA. More important, two ESTs present in the NCBI Database and corresponding to the 3′-untranslated region of the AOH3 transcript (BQ71452 and BQ898169) extend to the above-mentioned polyadenylation site. The 3′-sequence of the olfactory mucosa AOH3 cDNA is different from that of the corresponding mouse skin cDNA and is the result of a tissue-specific splicing event (see Table III).

The predicted open reading frame codes for a protein of 1345 amino acids and is slightly longer than that of AOX1, AOH1, and AOH2. This difference is mainly due to the insertion of an extra sequence in the hinge region located between the FAD and molybdenum cofactor domains of the protein and results from a change in the position of the splicing site of the junction of exons 15 and 16 (see below). The AOH3 amino acid sequence is easily aligned along its entire length with the sequences of the known mouse molybdo-flavoenzymes, as shown in Fig. 2. As all other members of the family (1), the N-terminal portion of AOH3 contains the conserved domains corresponding to the two non-identical iron-sulfur centers. In particular, AOH3 maintains the eight cysteine residues necessary for the coordination of the iron ions. These structural domains are followed by a relatively non-conserved hinge region that connects them to the ~45-kDa segment containing the FAD-binding site. The FAD-binding domain of AOH3 is characterized by a high level of amino acid identity to the corresponding domains of AOX1, AOH1, and AOH2, suggesting functional similarity. This domain is less conserved compared with the XOR counterpart, which can accommodate not only FAD, but also NAD (36, 37). Similar to what is observed in the case of AOX1, AOH1, and AOH2, the short sequence that is labeled by NAD derivatives in chicken XOR (38) and that is conserved in all XORs so far sequenced (1) is not present in AOH3. A second ill conserved hinge region precedes the 85-kDa molybdenum cofactor-containing and substrate-binding C-terminal domain of AOH3. In the last domain of AOH3, the signature sequence, (A/G)*XXX*(K/R/N/Q/H/T)X_{11-14}(L/I/V/M/F/Y/W/S)*XXXXXXXX*(L/I/V/M/F)*X*(C/F)*XX*(D/E/N)R*XX*(D/E) (1), of all molybdo-enzymes is evident.

Definition of the crystal structure of bovine XOR has led to the identification of Glu^{1261}, Arg^{880}, and Glu^{802}, residing in close proximity to the molybdenum active site, as fundamental residues in substrate recognition and enzyme catalysis (39). The equivalent amino acid residues in mouse XOR are Glu^{1264}, Arg^{883}, and Glu^{805} (1, 11, 18). Glu^{1264} is conserved in AOH3 (Glu^{1276}) and the other three mouse aldehyde oxidases, suggesting that the residue is important for the mechanisms of catalysis. The two charged amino acids Arg^{883} and Glu^{805} are substituted in AOH3 with the two neutral residues Phe^{895} and Val^{817}, respectively. This is similar to what is observed in mouse AOX1, AOH1, and AOH2. Consistent with the idea that Arg^{883} is important for the positioning of the hypoxanthine and xanthine rings in the molybdenum pocket, AOH3, like AOX1, AOH1, and possibly AOH2, does not utilize the two XOR substrates efficiently (see below).

Taken together, all of the structural characteristics of mouse AOH3 deduced from its primary sequence strongly indicate that the enzyme is a *bona fide* member of the molybdo-flavoprotein family. In addition, our data are consistent with the fact that AOH3 is more closely related to AOX1, AOH1, and AOH2 than to XOR. This, along with the enzymatic and genetic evidence outlined below, supports the notion that the protein belongs to the subgroup of aldehyde oxidases and justifies the name and the acronym adopted.

Cloning of the cDNAs Coding for the Rat AOH3, AOH2, and AOH1 Orthologous Proteins—Whereas putative orthologues of the AOX1 and XOR proteins have been identified in various vertebrate species (1), AOH1 and AOH2 have been described only in the mouse (14, 15, 34). The identification of the cDNA coding for AOH3 and the availability of the first draft of the rat genomes prompted us to verify the presence of sequences similar to the various mouse aldehyde oxidase homologues in this animal species. Computer analysis of the rat genome provided evidence for four aldehyde oxidase genes (NCBI accession number NW_047816), as in the mouse counterpart.

We cloned cDNAs containing the entire coding regions of rat AOH1, AOH2, and AOH3. Fig. 3 shows the alignment of the amino acid sequences deduced from the rat AOH1, AOH2, and AOH3 cDNAs with the corresponding mouse counterparts. Rat and mouse AOH3 are the two molybdo-flavoproteins that show the highest level of similarity (95%), followed by the AOH1 (90%) and AOH2 (89%) pair. These figures compare very well with the level of similarity observed in the case of rat and mouse AOX1 (93%) (17, 19) as well as rat and mouse XOR (94%) (11, 40). As expected, on the basis of what is known about the molybdo-flavoenzymes so far identified (1), rat AOH1, AOH2, and AOH3 are characterized by a high level of amino acid conservation in the N-terminal domains corresponding to the [2Fe-2S] redox centers. This includes conservation of the eight cysteines necessary for the coordination of the iron ions.

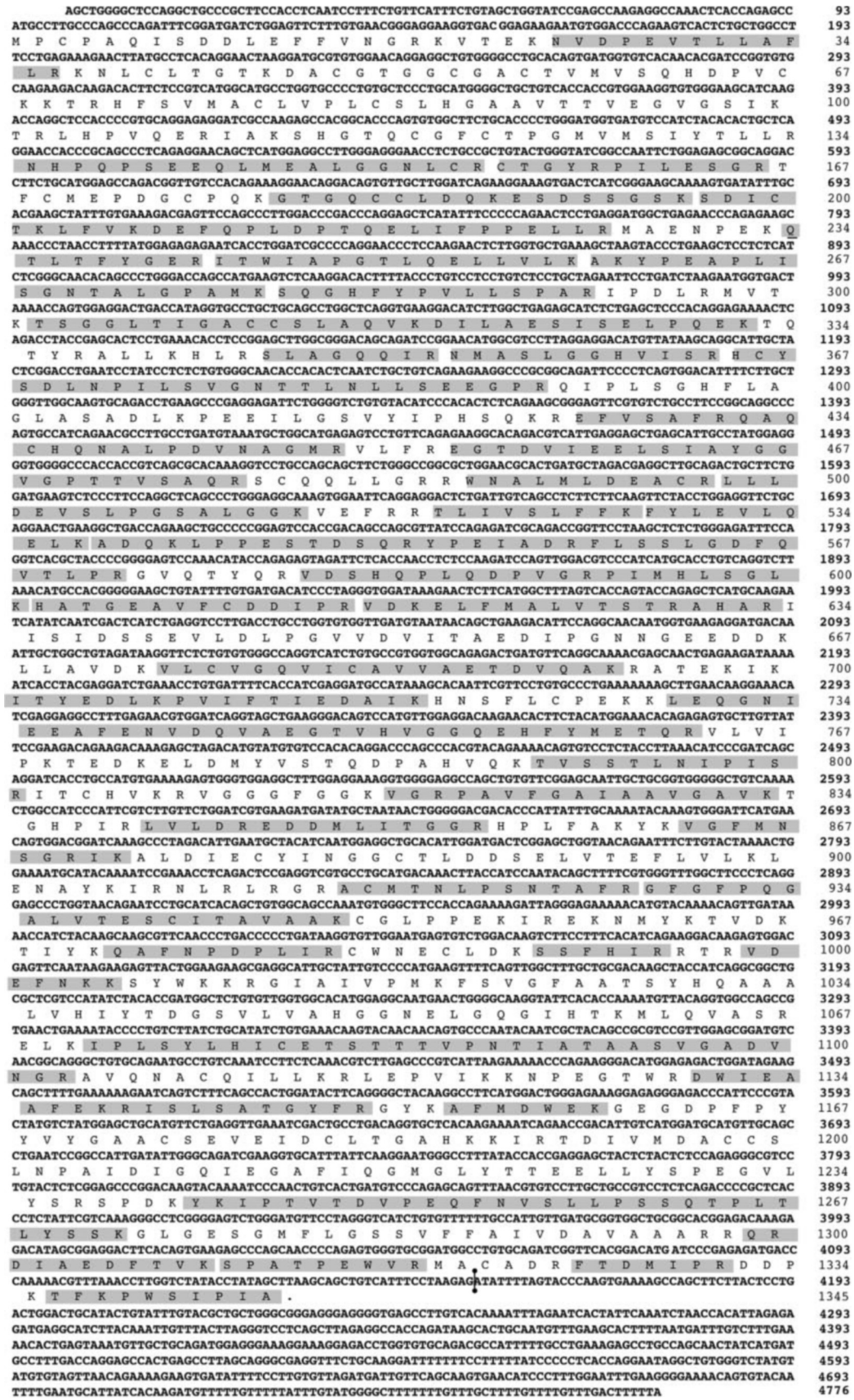

FIG. 1. **Nucleotide and deduced amino acid sequences of the cDNA of mouse olfactory mucosa AOH3.** The nucleotide sequence of the AOH3 cDNA (*upper line*) was obtained from overlapping cDNA fragments and is presented with its deduced amino acid sequence (*lower line*). Nucleotides are numbered in the 5′ → 3′ direction, whereas amino acids are numbered from the N terminus to the C terminus, starting from the putative first methionine residue. The sequences of the peptides obtained by tryptic digestion of purified olfactory mucosa AOH3 protein and identified by MALDI-TOF analysis are highlighted in *gray*. The *vertical line* dissecting the 3′-untranslated region of the cDNA marks the position at which the olfactory mucosa and skin AOH3 transcripts differ.

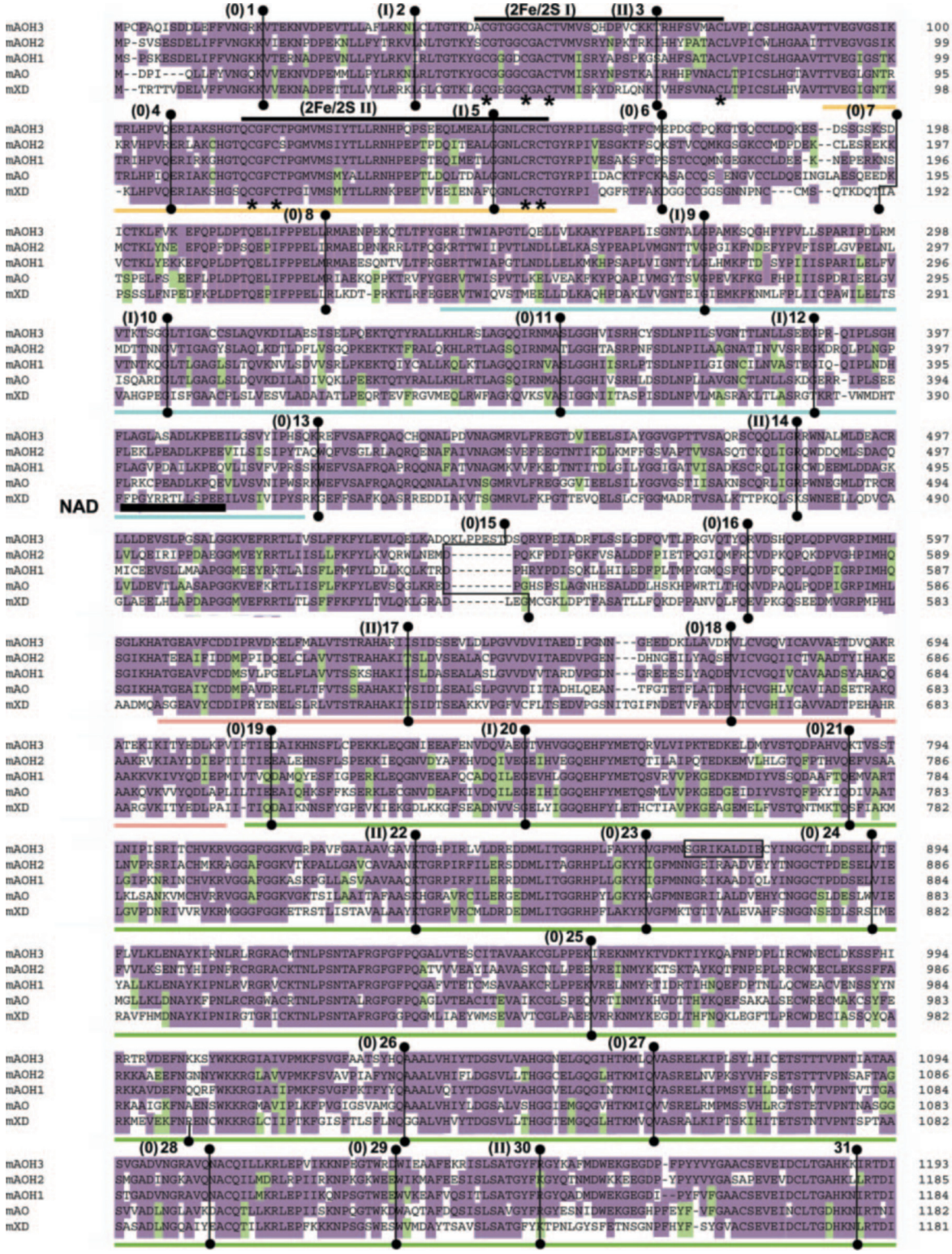

FIG. 2. **Amino acid sequence comparison of mouse AOH3, AOH2, AOH1, AOX1, and XOR.** The amino acid sequence of mouse (*m*) AOH3 is aligned with those of AOH2, AOH1, AOX1 (*mAO*), and XOR (*mXD*) using the ClustalW algorithm. Amino acid residues are numbered from the N terminus to the C terminus from the putative first methionine of each sequence. The residues highlighted in *magenta* represent identical amino acids relative to the AOH3 sequence. Identical amino acids present in sequences other than AOH3 are highlighted in *light green*. *Hyphens* represent gaps introduced to obtain the best alignment. The domains corresponding to the two non-identical [2Fe-2S] redox centers are *overlined*. In these domains, the *asterisks* below the sequences mark the positions of the cysteine residues reported to be involved in the formation of the iron-sulfur centers. The *thickly underlined* sequence of mouse XOR corresponds to the putative NAD^+-binding site, experimentally determined for chicken XOR. The color of the underlining indicates different domains of the proteins: *yellow*, [2Fe-2S] redox center-containing 25-kDa N-terminal domain; *light blue*, FAD-binding domain; *red*, hammerhead domain (Pfam 0315); *light green*, molybdenum cofactor- and substrate-binding domain. The *boxed* amino acid residues indicate the peptide used for the production of the anti-AOH3 antibody. The *vertical lines* connecting *two dots* indicate the positions of the exon/intron junctions of the corresponding genes. They are preceded by the exon number and the type of junction in *parentheses*.

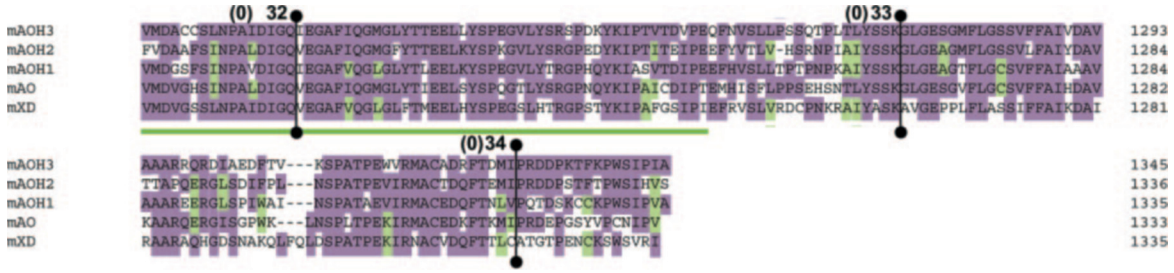

FIG. 2—*continued*

Equally conserved are the fingerprint sequences present in the 85-kDa substrate-binding regions of all molybdo-flavoenzymes. Interestingly, the fingerprint sequences of mouse and rat AOH3 are characterized by the presence of Leu at position 840. This substitutes for a very conserved cysteine present in XOR and AOX1 proteins of different origin and a phenylalanine in mouse or rat AOH1 and AOH2. Rat AOH1, AOH2, and AOH3 do not represent an exception to the rule with regard to the absence of Arg^{883} conserved in mouse and all other XOR proteins so far characterized. Similar to what is observed in the case of the mouse counterparts, this residue is changed to tyrosine or phenylalanine in rat AOH1, AOH2, and AOH3. Taken together, our data indicate that rats and mice express and synthesize the same complement of aldehyde oxidase proteins.

AOH3 Expression in the Olfactory Mucosa and Skin: Evidence for More than One AOH3 Transcript in the Olfactory Organ—The ethidium bromide staining of the agarose gel shown in Fig. 4*A* indicates that the only tissue demonstrating expression of the AOH3 transcript upon RT-PCR analysis of total RNA is the olfactory mucosa. The transcript was amplified from all other tissues considered, including the thymus and spleen, two organs of the immunological system that are rich in T- and B-lymphocytes, respectively. Small but detectable amounts of AOH3 mRNA were present also in the skin and were detected only upon enrichment of the RNA in the polyadenylated fraction. The tissue-specific profile of AOH3 expression is completely different from that of the other mouse molybdo-flavoenzymes, AOX1, AOH1, and XOR. In fact, AOX1 and AOH1 are co-localized in the hepatocytic component of the liver and in the alveolar septa of the lung, whereas the expression of XOR is relatively ubiquitous (11, 22). The tissue distribution of the AOH3 transcript partially overlaps with that of AOH2, which is expressed in the epidermal component of skin as well as in the keratinized epithelia of the oral cavity, esophagus and the first part of the stomach (14).

Sequencing of various AOH3 cDNA clones obtained from the olfactory mucosa and skin indicated the presence of different 3′-untranslated regions (3′-UTRs) in the two tissues. In particular, we observed that the nucleotide sequence of the last portion of the 3′-UTR of many AOH3 transcripts expressed in the olfactory mucosa is not represented in exon 35 of the *Aoh3* gene. Indeed, the last 617 nucleotides of the olfactory mucosa AOH3 transcript map to an extra exon (exon 36 downstream of exon 35 on mouse chromosome 1) (see Fig. 1 and Table III). As the nucleotide region lying between exon 35 and the putative exon 36 has not been sequenced completely, we determined the length of this stretch of genomic DNA by PCR analysis using a specific couple of amplimers corresponding to the two relevant exons. Exon 36 is located ~2.5 kilobase pairs downstream of exon 35. Inspection of the sequence of exon 35 indicates the presence of a potential GT splicing donor site next to the nucleotide marking the divergence between the 3′-UTRs of the AOH3 transcripts present in the skin and olfactory mucosa (see Table III). The GT dinucleotide is located 21 nucleotides downstream of the TAA stop codon of the AOH3 open reading frame. Conversely, inspection of the sequence of exon 36 demonstrates the presence of a putative AG splicing acceptor site adjacent to and upstream of the nucleotide marking the beginning of the olfactory mucosa-specific 3′-UTR. All this suggests that a differential splicing event is at the basis of the observed difference between the 3′-UTRs of the AOH3 mRNAs expressed in the olfactory mucosa and skin. To prove this hypothesis, we designed one common upstream amplimer corresponding to exon 34 (oligo 1) and three downstream amplimers corresponding to the common portion of exon 35 (oligo 2) as well as to the skin-specific region of exon 35 (oligo 3) and the olfactory-specific region of exon 36 (oligo 4). The amplimers were used in the RT-PCR experiments illustrated in Fig. 4*B*. As expected, a 131-bp band was amplified by oligo 1 and oligo 2 in both the skin and olfactory mucosa. Similarly, the combination of oligo 1 and oligo 3 allowed the amplification of a 257-bp cDNA fragment in the two tissues. In the case of the last combination (oligo1 and oligo 4), a specific RT-PCR band (420 bp) was observed only with RNA extracted from the nasal organ. This demonstrates that the olfactory mucosa expresses a mixture of AOH3 transcripts with different 3′-UTRs and contains tissue-specific factors capable of performing the differential splicing event necessary for the synthesis of the two distinct AOH3 mRNAs. The significance and functional consequences of this phenomenon are currently unknown.

The olfactory neuronal pathway consists of three main structures: the olfactory epithelium, the olfactory bulb, and the olfactory tuberculum. The olfactory epithelium is part of the olfactory mucosa, is located in the nasal cavities, and contains cells of neuronal origin that project their axons to the dorsal part of the olfactory bulb consisting of the intermediate neurons to which the odorant signals are conveyed. The last station of the pathway maps to a discrete and specialized structure, the olfactory tuberculum, where the stimuli are further elaborated before being relayed to other regions of the central nervous system. To evaluate the presence/absence of AOH3 and other members of the molybdo-flavoenzyme family in the various structures of the olfactory apparatus, Western blot experiments with monospecific antibodies were performed. As shown in Fig. 4*C*, a specific band of ~150 kDa corresponding to the monomeric subunit of AOH3 was evident in the cytosolic extracts obtained from the dissected olfactory epithelium. A similar band was undetectable in the cytosolic fractions of the olfactory bulb and tuberculum. The situation is similar to that of XOR, which was also expressed in the olfactory epithelium, but not in the bulb or tuberculum. In contrast, AOX1, AOH1, and AOH2 were not expressed at significant levels in any of the olfactory structures, whereas the three proteins were synthesized at high levels in the corresponding control tissues. Thus, our Western blot experiments indicate that AOH3 is present only in the most peripheral portion of the olfactory apparatus and that the only other molybdo-flavoprotein present in this anatomical structure is XOR.

The expression of mouse AOX1 and AOH1 is gender-specific,

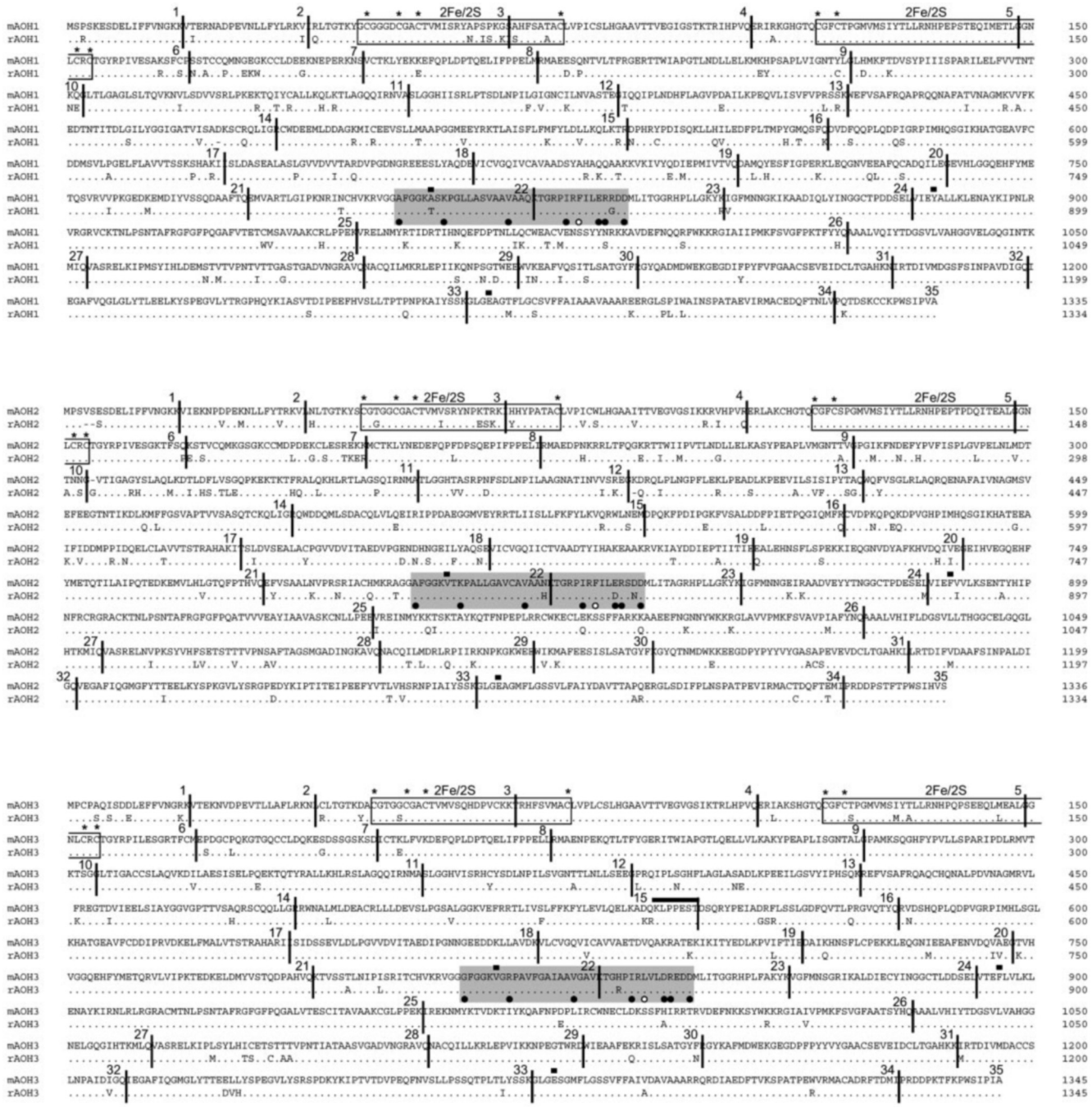

FIG. 3. **Amino acid sequence comparison of mouse and rat AOH1, AOH2, and AOH3.** The amino acid sequences of mouse (*m*) AOH1 (*upper*), AOH2 (*middle*), and AOH3 (*lower*) are aligned with those of the rat (*r*) counterparts using the ClustalW algorithm. Amino acid residues are numbered from the N terminus to the C terminus from the putative first methionine of each sequence. Identical amino acids with respect to the mouse counterpart in the rat sequence are indicated by *dots*. *Hyphens* represent gaps introduced to obtain the best alignment. Each exon is divided by *vertical bars* and numbered above the sequence. The domains corresponding to the two non-identical [2Fe-2S] redox centers are *boxed*. In these domains, the *asterisks* above the sequences mark the cysteine residues reported to be involved in the formation of the iron-sulfur centers. The fingerprint sequences observed in molybdenum-containing proteins are highlighted in *gray*. The *squares* above the sequences indicate the positions of the residues equivalent to Glu^{802}, Arg^{880}, and Glu^{1261} in bovine XOR (Glu^{805}, Arg^{883}, and Glu^{1264} in mouse XOR). The *black* and *white circles* below the sequences indicate highly conserved amino acids relative to the molybdo-flavoenzyme fingerprint sequence. The *thick line* above the amino acid sequence of AOH3 indicates the peptide that is uniquely present in AOH3, but not in AOH1 and AOH2 proteins.

as the two enzymes are expressed in higher amounts in the livers and lungs of male animals (14, 15, 34). Furthermore, the synthesis of AOX1, AOH1, and AOH2 is dependent on the mouse strain considered (34). Common mouse laboratory strains such as C57BL/6J (and CD1) contain relatively high amounts of AOH1 and lesser amounts of AOX1 in the liver (34). In contrast, equally common experimental mice such as DBA/2 and CBA are selectively and almost completely defective in the synthesis of AOH1 and synthesize significantly reduced amounts of AOX1 in the target organs (34). As demonstrated by the Western blot shown in Fig. 4*D*, the expected expression profile of AOH1 and AOX1 is evident in the livers of female and male C57BL/6J and DBA/2 mice. By contrast, the expression of AOH3 in the olfactory mucosa was influenced neither by the gender nor by the genetic background of the animals, as similar levels of the protein were present in both male and female C57BL/6J and DBA/2 mice. Our results indicate that only the genes coding for AOX1 and AOH1, but not those coding for

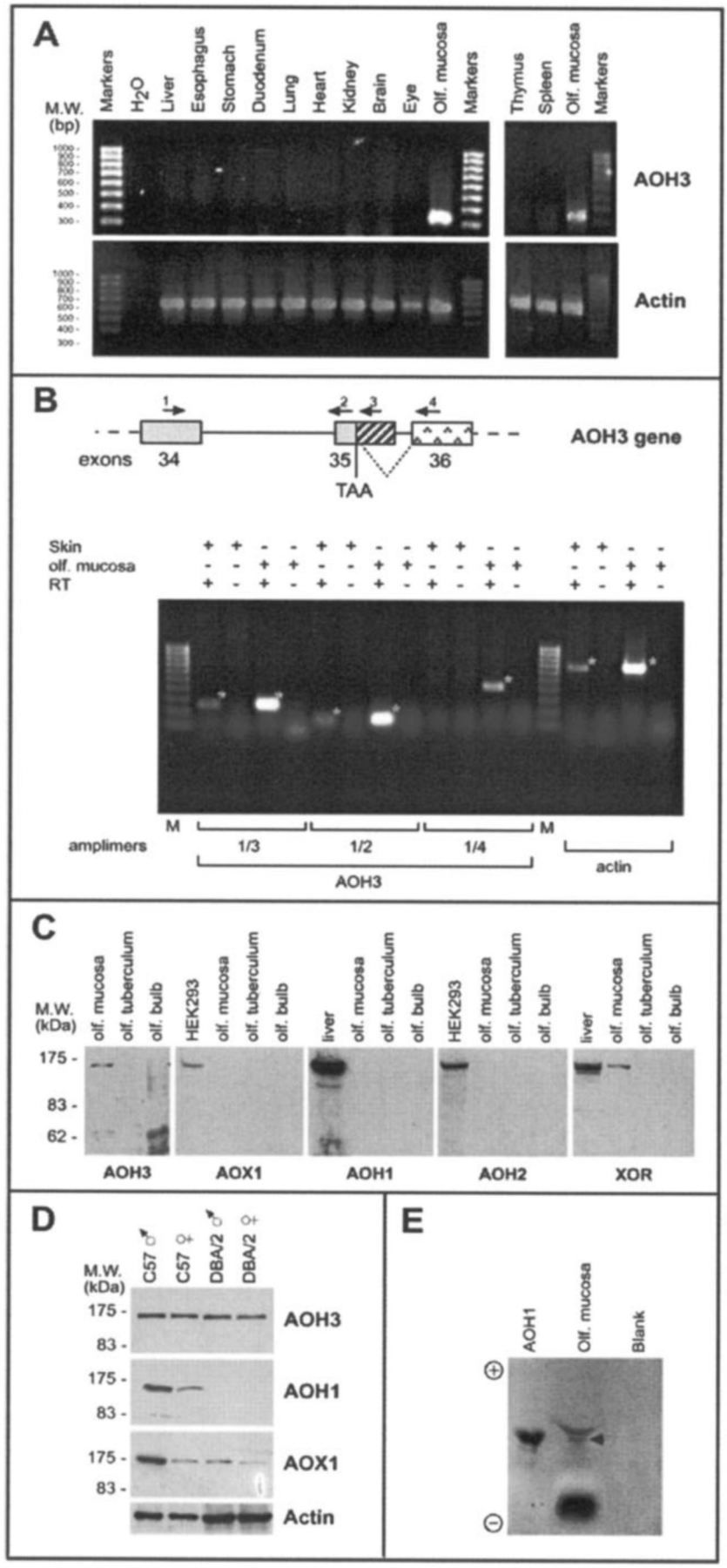

FIG. 4. **Tissue-specific expression of the AOH3 transcript and protein.** *A*, tissue distribution of the AOH3 transcript. Total RNA was obtained from the indicated tissues and used for RT-PCR analysis with AOH3-specific amplimers (5′-AAGACAAGACACTTCTCCGTCATG-3′, nucleotides 298–321; and 5′-TGTGGACAACCGTCTGGCTCCAT-3′, complementary to nucleotides 601–623). The amplified cDNA fragments were analyzed by 1% agarose gel electrophoresis. An actin cDNA fragment was also amplified to demonstrate that identical amounts of RNA from different tissues were used in the experiments. *B*, alternative splicing of AOH3 transcripts in skin and olfactory mucosa. The total RNA prepared from olfactory (*olf.*) mucosa and the poly(A^+) RNA from skin were used for RT-PCR analysis with amplimers 1–4, whose positions within the *Aoh3* gene are schematically shown (*upper*). The amplified DNA fragments obtained with the indicated combinations of amplimers were analyzed by 1% agarose gel electrophoresis and are shown (*lower*). The amplimers used were as follows: amplimer 1, 5′-GACTTCACAGTGAAGAGCCCAGCA-3′ (nucleotides 4006–4029); amplimer 2, 5′-GCTGCTTAAGCTATAGGTATAGACC-3′ (complementary to nucleotides 4112–4136); amplimer 3, 5′-CACAGCGATTTGAATGAACGCTTG-3′ (complementary to nucleotides 4260–4283; specific to the skin 3′-end and shown in Table III); and amplimer 4, 5′-CCCTCCATCTGCAGCAACATTTAC-3′ (complementary to nucleotides 4402–4425). *C*, expression of molybdo-flavoproteins in the olfactory system. Protein extracts were prepared from the indicated tissues or from HEK293 cells transfected with the AOX1 or AOH2 cDNA. Identical aliquots of cytosolic fractions (100 μg) were subjected to Western blot analysis with the indicated polyclonal antibodies. Molecular mass markers are listed on the left. *D*, gender and genetic background influence on the expression of molybdo-flavoenzymes. Cytosolic protein extracts were prepared from the olfactory mucosa and livers of male and female C57BL/6J and DBA/2 mice. Identical aliquots (100 μg) of the olfactory mucosa were subjected to Western blot analysis against anti-AOH3 and anti-actin antibodies, whereas liver extracts were challenged with anti-AOH1, anti-AOX1, and anti-actin antibodies. Molecular mass markers are listed on the left. *E*, benzaldehyde-oxidizing activity of olfactory mucosal extracts. Purified AOH1 (2 μg) or cytosolic extracts of olfactory mucosa (100 μg) were subjected to zymographic analysis following cellulose acetate electrophoresis using benzaldehyde as substrate.

AOH3 (as well as AOH2),[2] contain regulatory elements directly or indirectly responsive to testosterone and male sex hormones (17, 41–43). Furthermore, they suggest that epigenetic phenomena such as the hypermethylation of CpG dinucleotides observed in the regulatory elements of the *Aoh1* gene in DBA/2 mice (34) play a role in the expression of some (but not all) aldehyde oxidase genes.

Phthalazine is an excellent substrate for most of the mammalian aldehyde oxidases (34, 44) and is oxidized by AOH3 as well (see below). The zymogram shown in Fig. 4*E* demonstrates that the cytosolic fractions of homogenates obtained from the olfactory mucosa contained detectable levels of phthalazine-oxidizing activity. Upon electrophoresis on cellulose acetate plates, this activity was resolved into two bands. Under our experimental conditions, the phthalazine-oxidizing band corresponding to AOH3 had a mobility similar to that of purified mouse liver AOH1 (see also Fig. 6) and was clearly separated from the band corresponding to XOR, which did not migrate significantly on cellulose acetate plates. These results indicate that the AOH3 protein synthesized in the olfactory mucosa is catalytically active, at least as assessed with the artificial substrate phthalazine.

Cell-specific Expression of AOH3 in the Olfactory Mucosa—The olfactory mucosa consists of the olfactory epithelium, the basal lamina, and a subepithelial layer, where the glands (Bowman's glands) responsible for the production of the mucous fluid bathing the nasal cavities are located. To define the cell-specific distribution of AOH3 in the olfactory mucosa, we performed a number of *in situ* hybridization experiments using a cRNA probe recognizing the transcript coding specifically for this aldehyde oxidase isoform. The bright-field image in Fig. 5*A* shows a coronal section of the nasal cavities of a 10-day-old mouse. This is characterized by the presence of the olfactory epithelial layer, underneath which the large ducti of Bowman's glands are visible. Fig. 5*B* shows the dark-field image of an adjacent section of the nasal cavities. In this section, it is evident that the AOH3 mRNA is synthesized predominantly at the level of the canaliculi of Bowman's glands. The hybridization signal determined with the antisense AOH3 cRNA is specific, as the corresponding sense cRNA, used as a negative control, did not result in the accumulation of a significant number of silver grains on adjacent tissue slides (data not shown). Fig. 5*C* demonstrates that the accumulation of the silver grains corresponding to the AOH3 mRNA is at the level of the epithelial component of the canaliculi. Fig. 5*D* shows a sagittal section of the adult mouse olfactory mucosa consisting of the olfactory epithelium, the lamina propria, and the subepithelial layer, which is characterized by the presence of Bowman's glands and the corresponding ducti. The olfactory epithelium contains two main cell populations: the neuronal cells, which are specialized for the synthesis and expression of the odorant receptors, and the sustentacular cells, which exert a mechanical function. The sustentacular cells are believed to have the same origin as the cells constituting the ductal and parenchymal components of Bowman's glands (45). The dark-field photograph in Fig. 5*E* shows high levels of AOH3 mRNA expression in the subepithelial layer of the olfactory mucosa. In this region, the silver grain accumulation is consistent with the presence of the AOH3 transcript in the acinar and ductal components of Bowman's glands, as documented in Fig. 5*C*. AOH3 mRNA expression is evident also in the apical region of the olfactory epithelium, where the majority of sustentacular cells is located. The neuronal component of the olfactory epithelium is completely negative for the expression of AOH3.

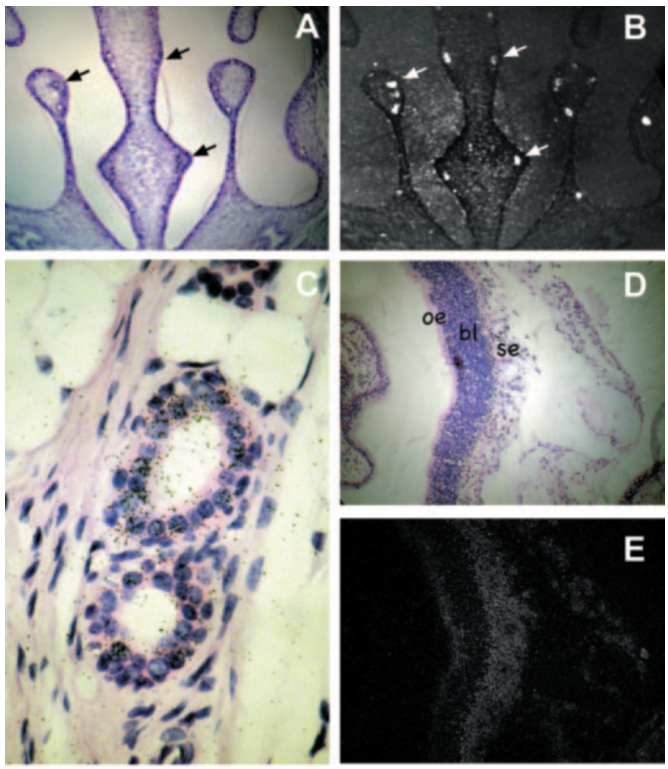

FIG. 5. **Cellular localization of mouse AOH3 in the olfactory mucosa.** A mouse AOH3 cRNA (nucleotides 72–2275) was synthesized *in vitro* from pAOH3-A in the presence of ^{35}S-labeled UTP. The resultant probe was hybridized on sections prepared from 10-day-old mouse whole nose preparations (*A–C*) and dissected adult mouse olfactory mucosa (*D* and *E*). The sections were stained with hematoxylin and eosin, and the corresponding bright-field (*A*, *C*, and *D*) and dark-field (*B* and *E*) images are presented. The *arrows* indicate the positions of Bowman's glands canaliculi. *oe*, olfactory epithelium; *bl*, basal lamina; *se*, subepithelial layer. Magnifications were ×100 (*A* and *B*; coronal sections), ×200 (*D* and *E*; sagittal sections) and ×1000 (*C*; coronal section).

Purification and Characterization of Mouse AOH3—To confirm the existence of AOH3 and to gain further insight into its structural and enzymatic properties, AOH3 was isolated from the olfactory mucosa. AOH3 was purified to homogeneity by ultracentrifugation, heat treatment, and subsequent ion exchange chromatography. Lack of an identified substrate for AOH3 prevented us from devising a simple and sensitive enzymatic assay to monitor the purification of the protein. Table I indicates that AOH3 is a relatively abundant protein in the olfactory mucosa. In fact, purification to homogeneity resulted in an overall enrichment of ~18-fold relative to the starting cytosolic preparation. The overall recovery of the protein was ~26% and was much higher than that obtained in the case of mouse liver AOX1 and AOH1 (14, 15, 34). This is probably the result of the fact that AOH3 purification does not require the extra affinity chromatography step on benzamidine-Sepharose that is necessary for the isolation of both AOX1 and AOH1 (15, 34). Typically, the absolute amounts of purified AOH3 recovered were on the order of 50–100 μg from 0.8 g of tissue (equivalent to ~100 animals). Fig. 6*A* shows results from the last purification step on an anion exchange column. AOH3 immunoreactivity centered around a symmetrical protein peak, indicating that the protein was pure. Fig. 6*B* shows that the chromatographic step separated AOH3 from XOR, the only other molybdo-flavoprotein coexpressed in the olfactory mucosa (see below). In fact, following elution with Mono Q and electrophoresis under denaturing and reducing conditions, the AOH3

[2] M. Kurosaki, M. Terao, M. M. Barzago, A. Bastone, D. Bernardinello, M. Salmona, and E. Garattini, unpublished data.

TABLE I
Purification of mouse AOH3

AOH3 was purified to homogeneity from the nasal epithelial mucosa of 100 mice. The purification of AOH3 was followed by quantitative Western blotting. The amounts of AOH3 protein determined following each purification step were quantitated by densitometry and are expressed in arbitrary units. The specific activity of the AOH3 protein isolated following each purification step was calculated by dividing the values in the third column by the corresponding values in the fourth column. The results shown are representative of three independent purification experiments.

Step	Volume	AOH3	Protein	Specific activity	Purification	Recovery
	ml	*arbitrary units*	*mg*	*units/mg protein*	*-fold*	*%*
Cytosol	2	44.8	5.6	8.0	1.0	100
55 PC	2	30.4	2.2	13.8	1.7	67
$(NH_4)_2SO_4$	1	31.8	1.0	31.8	4.0	71
Mono Q	2	11.6	0.08	145.7	18.2	26

protein was recognized by the anti-AOH3 antibody, but not by the anti-XOR antibody. Fig. 6*C* demonstrates that the AOH3 preparation was indeed homogeneous, as it consisted of a single band of ~150 kDa upon denaturing and reducing PAGE and Coomassie Blue staining. To establish its identity to AOH3, the purified protein band was trypsinized following reduction and carboxymethylation, and the tryptic digest was subjected to MALDI-TOF mass spectrometry. As illustrated in Fig. 6*D*, the spectrum was entirely different from that of the other mouse molybdo-flavoprotein, AOH1, which we purified from CD1 and DBA/2 mouse livers.

Table II demonstrates that 48 peptides generated from the purified AOH3 protein could be unequivocally identified on the basis of the masses of the tryptic fragments predicted from the open reading frame of the cloned AOH3 cDNA. Other peptides listed are likely to be mixtures of two or three peptides with equivalent masses. For all peptides identified, the difference between the calculated and experimentally determined masses is <0.05 mass units. Altogether, the identified peptides cover ~50% of the entire sequence of mouse AOH3 (Fig. 1). A computer-assisted search in the NCBI Database using the masses determined for the 25 most abundant identified peaks did not result in any significant hit. This demonstrates that the protein band purified from the olfactory mucosa corresponds to mouse AOH3. The sequences of some of these peptides were determined directly by *de novo* sequencing with tandem mass spectrometry, confirming the results obtained by MALDI-TOF analysis.

As demonstrated by the zymographic analysis shown in Fig. 6*D*, AOH3 is a catalytically active enzyme and oxidizes phthalazine, benzaldehyde, retinaldehyde, octanal, and 2-OH-pyrimidine, five known substrates of AOX1 and AOH1 (34). Upon cellulose acetate electrophoresis, purified AOH3 migrated toward the cathode with a mobility similar to that of purified mouse AOH1, which was used as a positive control in these experiments. Although AOH3 has the potential to oxidize the five above-mentioned substrates, it did so much less efficiently than AOH1. In fact, similar amounts of AOH1 were much more active in utilizing the selected substrates to reduce the indicator chromophore 3-(4,5-dimethylthiazol-2-yl)-2,5-diphenyltetrazolium bromide, suggesting that the substrate specificity of AOH3 and AOH1 is similar, but that the catalytic efficiency is different. In addition, our results suggest that phthalazine is the best substrate for AOH3 among the limited series of compounds considered. Regardless of these details, it is evident that AOH3, like AOX1 and AOH1, oxidizes artificial substrates containing aldehydes and *N*-heterocycles. Interestingly and unlike XOR, the band corresponding to purified AOH3 was devoid of detectable hypoxanthine-oxidizing activity (data not shown). This indicates that the novel molybdo-flavoprotein has low affinity for this substrate and suggests that AOH3 is more closely related to AOX1, AOH1, and AOH2 than to XOR not only in terms of structure, but also in terms of substrate preference.

Aldehyde Oxidase Gene Clusters in Mouse and Rat—Sequencing of the mouse AOH3 cDNA as well as the rat AOH1, AOH2, and AOH3 cDNAs made it possible to unequivocally identify the exon/intron boundaries of the corresponding genes. As schematized in Fig. 7, mouse *Aoh3* is located ~10 kilobase pairs from exon 35 of *Aoh2*, which positions the novel gene on chromosome 1 band c1 within the context of the previously identified aldehyde oxidase gene cluster (15). Hence, the mouse gene cluster consists of the four genes *Aox1*, *Aoh1*, *Aoh2*, and *Aoh3*, which are located a short distance from one another and which are transcribed from the same DNA strand and in the same orientation. A similar arrangement of the *Aox1*, *Aoh1*, *Aoh2*, and *Aoh3* orthologues is evident on chromosome 9q31 of the rat genome. The DNA sequences separating the rat *Aox1*, *Aoh1*, *Aoh2*, and *Aoh3* genes are of similar lengths to those of the corresponding mouse counterparts. The relative lengths of the mouse and rat aldehyde oxidase gene orthologues are similar and vary from ~55 kilobase pairs in the case of *Aoh2* to ~90 kilobase pairs in the case of *Aoh1*.

The exon/intron structure of the mouse *Aoh3* gene is shown in Table III. The *Aoh3* gene is at least 80 kilobase pairs long, consists of 35 coding exons, and has the potential to transcribe an extra noncoding exon (exon 36) representing the last portion of the 3′-untranslated region of the transcript expressed in the olfactory mucosa through an alternative splicing event (see above). With respect to this last point, it remains to be established whether a similar situation applies also to the rat *Aoh3* orthologue. Except for intron 2, which begins with an unusual GG dinucleotide, all of the exon/intron junctions of the mouse *Aoh3* gene conform to the GT/AG consensus sequence found in other eukaryotic genes. Given the high level of similarity at the cDNA and protein levels, it is not surprising that this is true also in the case of the rat *Aoh3*, *Aoh2*, and *Aoh1* genes. With the exception of the junction between exons 15 and 16, the positions and types of all of the coding exon boundaries of the mouse *Aoh3* gene are conserved in mouse *Aox1*, *Aoh1*, and *Aoh2*, as indicated in Fig. 2. Furthermore, 33 of 35 junctions are identical in mouse *Aoh3*, *Aoh2*, *Aoh1*, *Aox1*, and *Xor*. As expected, perfect conservation of the exon/intron junctions is evident in the mouse and rat *Aoh3*, *Aoh2*, and *Aoh1* (Fig. 3) (15), *Aox1* (46), and *Xor* (18) orthologues. The splicing junction of exon 15/16 is different in mouse *Aoh3* relative to all other members of the family. This is the result of the fact that exon 15 is 21 nucleotides longer than the corresponding exons in *Aox1*, *Aoh1*, *Aoh2*, and *Xor* and codes for seven extra amino acids (KLPPEST). Although the KLPPEST sequence falls within the predicted hinge region connecting the 45-kDa FAD domain with the 85-kDa molybdenum cofactor domain, it may have significance for the structure/function of the AOH3 protein. In fact, the exon 15/16 splicing junction of mouse *Aoh3* is maintained in the rat counterpart, which results in the synthesis of a protein with a conserved KLPPEST sequence (Fig. 3). As already noticed for mouse *Aox1*, *Aoh1*, *Aoh2*, and *Xor*, even in the case of mouse *Aoh3* as well as rat *Aoh1*, *Aoh2*, and

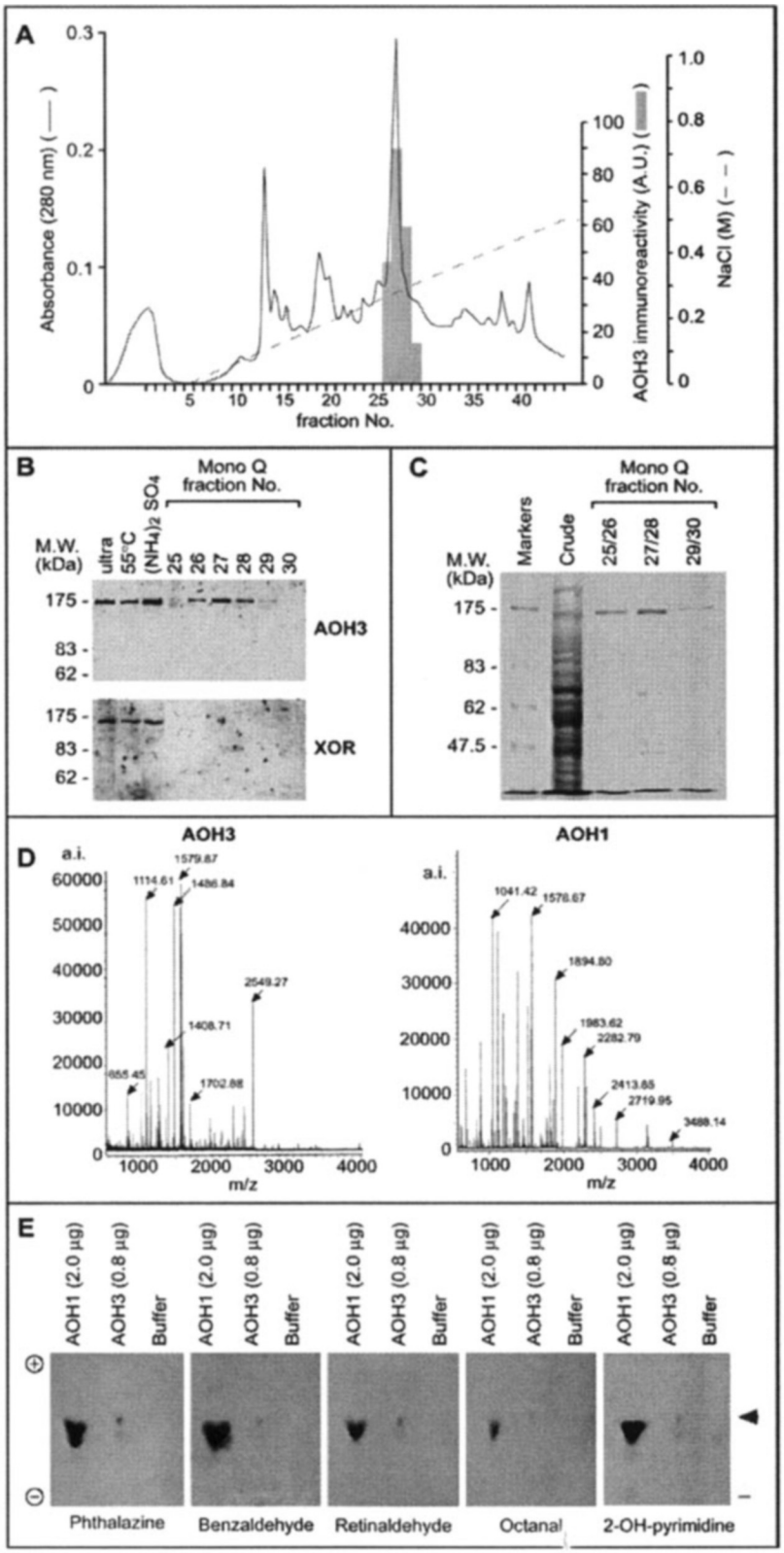

FIG. 6. **Purification and characterization of mouse epithelial mucosa AOH3.** *A*, Mono Q ion exchange chromatography of mouse epithelial mucosa AOH3. The protein fraction precipitated by ammonium sulfate (~1 mg of protein) was applied to a Mono Q fast protein liquid chromatography column and eluted with a linear gradient of NaCl as indicated (*dashed line*). The column was run at a flow rate of 0.5 ml/min, and 1-min fractions were collected. An aliquot of each chromatographic fraction was assayed for the presence of AOH3 immunoreactivity using quantitative Western blot analysis, and the corresponding elution profile is indicated by the *shaded columns* superimposed over the protein profile monitored at 280 nm. *A.U.*, arbitrary units. *B*, samples obtained from the indicated purification steps or aliquots of the specified Mono Q chromatographic fractions were subjected to Western blotting using specific anti-AOH3 and anti-XOR polyclonal antisera. The positions of appropriate protein molecular mass markers are indicated on the left. *ultra*, cytosolic extract of olfactory mucosa; *55 °C*, cytosolic extract following treatment for 10 min at 55 °C; *$(NH_4)_2SO_4$*, ammonium sulfate cut of heated cytosolic extracts. *C*, aliquots from the specified pooled fractions of the Mono Q chromatographic step shown in *A* were stained with Coomassie Blue. The Coomassie Blue staining of the initial crude extract obtained from the olfactory epithelium is shown for comparison. Protein molecular mass markers and the corresponding apparent masses are shown on the left. *D*, tryptic peptides derived from the AOH3 and AOH1 proteins purified from mouse epithelial mucosa and liver, respectively, were analyzed by MALDI-TOF mass spectrometry. *a.i.*, adjusted intensity. *E*, purified AOH3 and AOH1 were analyzed by zymography with the indicated substrates (10 mM). The amounts of purified AOH3 and AOH1 are indicated in *parentheses*. The *arrowhead* indicates the position of the enzymatic activity corresponding to AOH3. The *line* on the right indicates the loading position of the samples.

Aoh3, the type (0, I, or II) of intron-exon junctions are strictly conserved. The striking conservation of the exon/intron junctions represents compelling evidence that AOH3 has the same genetic origin as all other members of the molybdo-flavoenzyme family and evolved from the same ancestral precursor.

It is believed that single coding exons often define functional or structural domains of modular proteins. Although the two species are phylogenetically close, comparison of the coding exon sequences of the *Aoh3*, *Aoh2*, *Aoh1*, *Aox1*, and *Xor* genes in mouse and rat gives a unique opportunity to obtain insight into the structural/functional significance of the polypeptide regions defined by single exons in each molybdo-flavoenzyme. With this in mind, we first calculated the mean value of similarity of the coding exons of each mouse/rat molybdo-flavoenzyme gene couple. As shown in Table IV, this value is highest in the case of *Aoh3*, followed by *Xor*, *Aox1*, *Aoh1*, and *Aoh2*.

TABLE II

MALDI-TOF analysis of tryptic peptides from purified AOH3 and electrospray ionization tandem mass spectrometry sequencing of selected tryptic peptides

AOH3 protein purified from mouse olfactory mucosa was trypsinized and subjected to MALDI-TOF mass spectrometric analysis. For MALDI-TOF mass spectrometry (MS), the analysis was limited to tryptic peptides with a molecular mass equal to or more than 700 Da. For MALDI-TOF analysis, the data in the first column are the mass values obtained experimentally (observed (obs)). The results in the second column are those calculated (cal) from the *in silico* tryptic fragmentation of the *Aoh3* gene product. The third column indicates the amino acid positions of the identified AOH3 peptides. The fourth column shows the corresponding amino acid sequences. The single asterisks indicate methionine sulfoxide modification, and the double asterisks indicate carboxyamidomethylcysteine modification. For electrospray ionization tandem mass spectrometry (ESI-MS/MS), the data in the first column are the m/z values obtained experimentally. The second column shows the charge state of each peptide. The third column illustrates the *de novo* sequencing results along with the residue positions.

MALDI-MS $M+H^+$ obs	$M+H^+$ cal	Identification	Sequence
746.42	746.39	990-995	SSFHIR
855.45	855.44	425-431	EFVSAFR
867.44	867.41	863-870	VGFMNSGR
883.41	883.41 *	863-870	VGFMNSGR
872.48	872.49	345-352	SLAGQQIR
879.46	879.46	999-1005	VDEFNKK
879.46	879.44	1325-1331	FTDMIPR
926.41	926.41	1153-1159	AFMDWEK
1042.56	1042.53	1310-1318	SPATPEWVR
1067.66	1067.65	519-527	TLIVSLFFK
1108.55	1108.53 or/and 1108.59	1130-1138 or/and 863-872	DWIEAAFEK or/and VGFMNSGRIK
1114.61	1114.55 or/and 1114.59	234-242 or/and 1140-1149	QTLTFYGER or/and ISLSATGYFR
1153.63	1153.63	197-206	SDICTKLFVK
1159.66	1159.65	1336-1345	TFKPWSIPIA
1170.66	1170.73	972-981	QAFNPDPLIR
1241.67	1241.64	353-364	NMASLGGHVISR
1264.67	1264.63	1130-1139	DWIEAAFEKR
1267.70	1267.67	619-629	ELFMALVTSTR
1270.75	1270.69	1139-1149	RISLSATGYFR
1281.73	1281.71	528-537	FYLEVLQELK
1287.76	1287.73	790-801	TVSSTLNIPISR
1321.70	1321.60	487-497	WNALMLDEACR
1378.65	1378.62 **	487-497	WNALMLDEACR
1408.73	1408.70 **	155-166	CTGYRPILESGR
1482.71	1482.68 **	915-927	ACMTNLPSNTAFR
1486.84	1486.83	24-36	NVDPEVTLLAFLR
1568.87	1568.89	498-513	LLLDEVSLPGSALGGK
1571.84	1571.77 or/and 1571.82 or/and 1571.83	538-551 or/and 319-332 or/and 279-292	ADQKLPPESTDSQR or/and DILAESISELPQEK or/and SQGHFYPVLLSPAR
1579.87	1579.85	559-572	FLSSLGDFQVTLPR
1582.96	1582.94	817-833	VGRPAVFGAIAAVGAVK
1587.75	1587.72 **	602-615	HATGEAVFCDDIPR
1609.88	1609.86	616-629	VDKELFMALVTSTR
1625.86	1625.86 *	616-629	VDKELFMALVTSTR
1702.88	1702.88 or/and 1702.91	840-854 or/and 619-633	LVLDREDDMLITGGR or/and ELFMALVTSTRAHAR
1718.88	1718.87 * or/and 1718.90 *	840-854 or /and 619-633	LVLDREDDMLITGGR or/and ELFMALVTSTRAHAR
1794.80	1795.07	243-258	ITWIAPGTLQELLVLK
1829.93	1829.76 or/and 1829.95	179-196 or/and 261-278	GTGQCCLDQKESDSSGSK or/and YPEAPLISGNTALGPAMK
1909.89	1909.88 **	432-448	QAQCHQNALPDVNAGMR
1973.94	1973.96	542-558	LPPESTDSQRYPEIADR
1993.97	1994.20	243-260	ITWIAPGTLQELLVLKAK
2029.06	2029.08	259-278	AKYPEAPLISGNTALGPAMK
2045.07	2045.08	674-693	VLCVGQVICAVVAETDVQAK
2108.14	2108.15	701-718	ITYEDLKPVIFTIEDAIK
2124.07	2124.08 **	928-948	GFGFPQGALVTESCITAVAAK
2280.06	2280.05 **	135-154	NHPQPSEEQLMEALGGNLCR
2397.24	2397.23	207-226	DEFQPLDPTQELIFPPELLR
2424.29	2424.26 or/and 2424.28	552-572 or/and 580-601	YPEIADRFLSSLGDFQVTLPR or/and VDSHQPLQDPVGRPIMHLSGLK
2440.27	2440.28 *	580-601	VDSHQPLQDPVGRPIMHLSGLK
2549.27	2549.27	453-477	EGTDVIEELSIAYGGVGPTTVSAQR
2705.16	2705.27 *	425-448	EFVSAFRQAQCHQNALPDVNAGMR
2884.48	2884.55	203-226	LFVKDEFQPLDPTQELIFPPELLR
2899.38	2899.43 **	365-390	HCYSDLNPILSVGNTTLNLLSEEGPR
3161.55	3161.61 or/and 3161.66	302-332 or/and 1244-1272	TSGGLTIGACCSLAQVKDILAESISELPQEK or/ and IPTVTDVPEQFNVSLLPSSQTPLTLYSSK
3429.59	3429.73 **	1071-1103	IPLSYLHICETSTTTVPNTIATAASVGADVNGR
3452.59	3452.82	1242-1272	YKIPTVTDVPEQFNVSLLPSSQTPLTLYSSK
3990.48	3990.82	729-763	LEQGNIEEAFENVDQVAEGTVHVGGQEHFYMETQR

ESI-MS/MS $M+H^+$ obs	Charge state	Sequence
558.31	2+	ISLSATGYFR (1140-1149)
744.45	2+	NVDPEVTLLAFLR (24-36)
787.47	2+	DILAESISELPQEK (319-332)
790.46	2+	FLSSLGDFQVTLPR (559-572)
1267.71	1+	ELFMALVTSTR (619-629)

Subsequently, we determined the exons of each gene couple showing a level of similarity significantly higher (above the 95th percentile of the distribution) and lower (below the 5th percentile of the distribution) than the corresponding mean value. We reasoned that the first set of exons, which we termed hyperconserved exons, are under selective pressure because they are translated into peptide domains of functional or structural relevance for the encoded molybdo-flavoenzyme. In contrast, the second set of exons, which we termed hypervariable exons, are likely to code for stretches of amino acids that are not essential for the structure/function of the molybdo-flavoenzyme considered. As shown in Table IV, numerous exons fall within the range of the hyperconserved group, whereas only few are of the hypervariable type. Exons 21, 23, 25, and 27 are hyperconserved in all molybdo-flavoenzyme genes, suggesting that they code for important and general structural or functional determinants of the corresponding class of enzymes. All these exons code for domains contained in the molybdenum cofactor- and substrate-binding regions of the molybdo-flavoproteins. On the other hand, exon 35 is specific to the aldehyde oxidase genes, *Aox1*, *Aoh1*, *Aoh2*, and *Aoh3*, which indicates the presence of a determinant discriminating between XOR and all other members of the mammalian molybdo-flavoprotein family. The *Aox1*/*Aoh2* and *Aoh1*/*Aoh2* couples do not

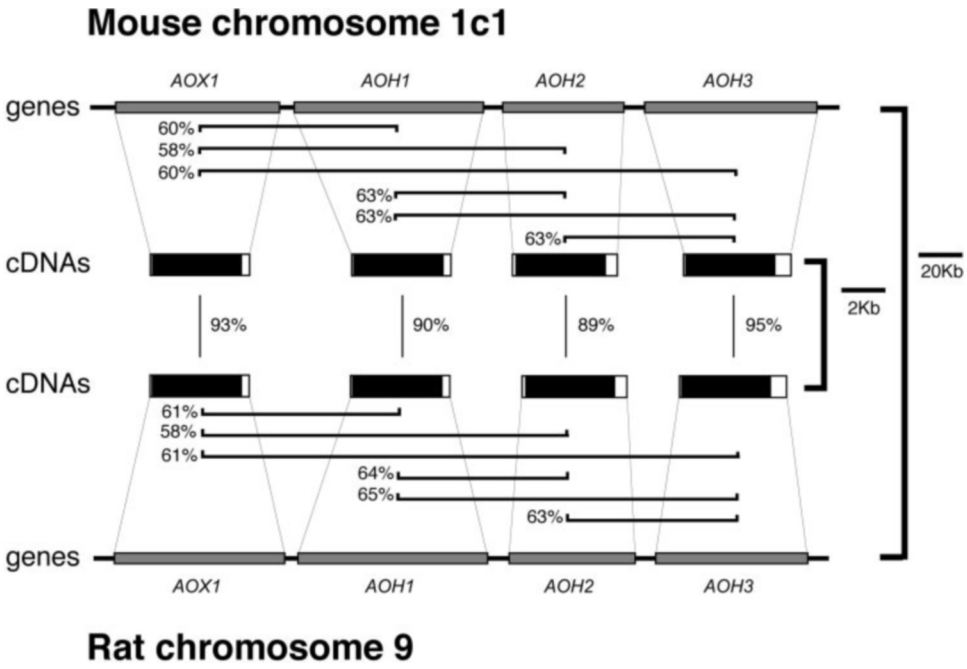

FIG. 7. **Physical map of the mouse and rat *Aox1*, *Aoh1*, *Aoh2*, and *Aoh3* loci.** The relative positions of the *Aox1*, *Aoh1*, *Aoh2*, and *Aoh3* genetic loci on mouse chromosome 1 band c1 (*upper*) and rat chromosome 9 (*lower*) are schematized. The *gray boxes* represent the indicated genes, and the *thick lines* represent the flanking sequences. The *black* and *white boxes* indicate the coding and noncoding sequences of the cDNAs, respectively. The percent similarities at the amino acid level between various oxidases are also indicted.

share hyperconserved exons. Exons 9 and 10 are hyperconserved only in *Aoh3*, whereas exons 7 and 26 are hyperconserved only in *Xor*. These may represent exons coding for structural domains specific for each molybdo-flavoenzyme. Similarly, exons 1 and 20 are hyperconserved only in *Aoh1* and *Aox1*, respectively. Interestingly, the hyperconserved domains of *Aoh3* are contained in the FAD-binding region of the protein, whereas the one present in *Aox1* belongs to the molybdenum cofactor- and substrate-binding region. Exons 1, 7, 13, and 16 are hypervariable in one or more of the various molybdo-flavoenzyme genes. Perhaps, it is not surprising that exon 7 is hypervariable in *Aox1*, *Aoh1*, and *Aoh2*, as it codes for part of the hinge region connecting the second [2Fe-2S] and the FAD-binding domains.

DISCUSSION

The main findings of this work are the identification and characterization of rodent AOH3, a novel member of the molybdo-flavoenzyme family endowed with aldehyde oxidase activity, as well as the definition of the structure of the entire aldehyde oxidase gene cluster in mouse and rat. The identification of AOH3 raises the number of mammalian molybdo-flavoenzymes to five.

Selective Localization of AOH3, a Typical Molybdo-flavoenzyme, in the Olfactory Mucosa—Sequencing of the entire mouse genome and release of the first draft of the rat counterpart facilitate the identification of novel open reading frames coding for potential proteins. *In silico* analysis of the two genomes allowed us to identify orthologous genes coding for AOH3, a novel member of the molybdo-flavoprotein family. The two orthologous genes are expressed in the form of a specific polyadenylated mRNA in mouse and rat, as assessed by cloning of the corresponding cDNAs. In addition, the mouse AOH3 transcript is translated into a biologically active enzyme that can be purified to homogeneity from the olfactory mucosa. Sequencing of the mouse and rat cDNAs demonstrated that the encoded proteins have the typical structural features of the monomeric subunits of mammalian molybdo-flavoenzymes, including the presence of two non-identical [2Fe-2S] redox centers, a FAD domain, and a molybdenum cofactor domain (1). Although, at present, there is no direct evidence that AOH3, like all other members of the molybdo-enzyme family, is a dimer of the monomeric subunit, it is likely that this is the case. In fact, several amino acids involved in the dimerization of bovine XOR are conserved in mouse and rat AOH3. Definition of the amino acid sequence of AOH3 indicates that the protein is more similar to mouse and rat AOX1, AOH1, and AOH2 than to the other molybdo-flavoenzyme, XOR. This suggests that the novel molybdo-flavoenzyme can be functionally classified as a molybdenum-containing aldehyde oxidase. This classification is supported by the following evidence. AOH3, like mouse and rat AOX1, AOH1, and AOH2 as well as aldehyde oxidases of insect (1, 47, 48) and plant (49–51) origin, lacks the Glu residue (Glu^{803}) present in the substrate-binding site of bovine XOR and conserved in all other XORs so far characterized. This residue is of fundamental importance for the catalysis of XOR, as it positions the specific substrates, xanthine and hypoxanthine, into the substrate pocket of the enzyme. As expected on the basis of this last structural characteristic, mouse AOH3, like AOX1, AOH1, and AOH2, does not oxidize hypoxanthine and xanthine to a significant level. More important, purification of AOH3 from the mouse epithelial mucosa demonstrated that the enzyme possesses aldehyde oxidase activity, as it oxidizes various aromatic and aliphatic aldehydes as well as heterocycles like phthalazine, which are recognized substrates of both AOX1 and AOH1 (34). Although purified AOH3 seems to oxidize these substrates less efficiently than AOH1 (this study) and AOX1,[2] it is currently difficult to identify the reasons underlying this phenomenon. It is possible that the enzyme has a lower affinity for these substrates than the other members of the mammalian aldehyde oxidase family. However, it is equally possible that AOH3 is only partially active because a proportion of the purified enzyme is in its desulfo or demolybdo form, as observed in the case of purified milk XOR (52, 53). Currently, the limited amounts of native AOH3 that can be recovered from the olfactory mucosa hamper a more thorough analysis of the biochemical and structural characteristics of the enzyme.

TABLE III

Exon/intron organization of the mouse Aoh3 gene

Exon sequences are in uppercase letters, and intron sequences are in lowercase letters. The positions of nucleotides close to the 5′- and 3′-ends of the exons are numbered below the DNA sequence. Nucleotide numbering is the same as that of the AOH3 cDNA sequence. Amino acids bordering the splice junctions are shown above the nucleotide sequence. The sequence in exon 35 that serves as an alternative splice donor site is shown as a gt dinucleotide in lowercase letters.

Ex	Ex Size (bp)	5′-splice site	Intr Size (bp)	3′-splice site	Ex	Ex Size (bp)	5′-splice site	Intr Size (bp)	3′-splice site
1	150	..Gly Arg Lys ..GGG AGG AAGgtaagtttct.. 142	2.7	Val Thr Glu.. .. tccaatgcagGTG ACG GAG.. 151	19	123	..Thr Ile Glu ..ACC ATC GAGgtaagctggg.. 2227	9.0	Asp Ala Ile.. ..ttttgcacagGAT GCC ATA.. 2236
2	58	..Lys Asn L ..AAG AAC Tggacccttct.. 202	1.4	eu Cys Leu.. ..tccttcccagTA TGC CTC.. 209	20	97	..Ala Glu G ..GCT GAA Ggtaagtagta.. 2326	9.0	ly Thr Val.. ..cccctcacagGG ACA GTC.. 2333
3	97	..Lys Thr Ar ..AAG ACA AGgtagctaccc.. 298	0.7	g His Phe.. ..ccacacaaagA CAC TTC.. 306	21	125	..His Val Gln ..CAC GTA CAGgtaagatcca.. 2449	1.6	Lys Thr Val.. ..tctcttacagAAA ACA GTG.. 2458
4	109	..Pro Val Gln ..CCC GTG CAGgtaagcacac.. 406	2.0	Glu Arg Ile.. ..atgcttccagGAG AGG ATC.. 415	22	134	..Ala Val Ly ..GCT GTC AAgtaagtctac.. 2584	2.0	e Thr Gly.. ..ttttctgcagA ACT GGC.. 2592
5	127	..Leu Gly G ..TTG GGA Ggtaggtgtga.. 535	2.0	ly Asn Leu.. .. ctctgatcagGG AAC CTC.. 542	23	88	..Lys Tyr Lys ..AAA TAC AAAgtaagtgcta.. 2671	1.8	Val Gly Phe.. ..tcggcgacagGTG GGA TTC.. 2680
6	62	..Phe Cys Met ..TTC TGC ATGgtgagtacac.. 595	2.2	Glu Pro Asp.. ..atgtcctcagGAG CCA GAC.. 604	24	87	..Ser Glu Leu ..TCG GAG CTGgtatgtgtgt.. 2758	0.6	Val Thr Glu.. ..ttttctttagGTA ACA GAA.. 2767
7	84	..Lys Ser Asp ..AAA AGT GATgtgagtccct.. 679	2.2	Ile Cys Thr.. ..ttttataaagATT TGC ACG.. 688	25	192	..Pro Glu Lys ..CCA GAA AAGgtaagattat.. 2950	1.9	Ile Arg Glu.. ..cttgtttcagATT AGG GAG.. 2959
8	81	..Glu Leu Leu ..GAA CTC CTGgtaagacaac.. 760	2.0	Arg Met Ala.. ..ttgccctcagAGG ATG GCT.. 769	26	228	..Tyr His Gln ..TAC CAT CAGgtaaagttca.. 3178	4.0	Ala Ala Ala.. ..tttcccacagGCG GCT GCG.. 3187
9	145	..Ala Leu G ..GCC CTG Ggtaagtggtc.. 907	1.4	ly Pro Ala.. ..tttccttcagGA CCA GCC.. 914	27	96	..Met Leu Gln ..ATG TTA CAGgtaaaatcaa.. 3274	2.5	Val Ala Ser.. ..tttctcacagGTG GCC AGC.. 3283
10	93	..Ser Gly G ..AGT GGA Ggtaagttccag.. 1000	3.8	ly Leu Thr.. ..tgctcttccagGA CTG ACC.. 1007	28	129	..Ala Val Gln ..GCT GTG CAGgtgactgctc.. 3403	2.7	Asn Ala Cys.. ..tttcttctagAAT GCC TGT.. 3412
11	152	..Asn Met Ala ..AAC ATG GCGgtgggtctcc.. 1150	0.7	Ser Leu Gly.. ..ctctctctagTCC TTA GGA.. 1159	29	75	..Arg Asp Trp ..AGA GAC TGGgtaggtgctc.. 3478	1.1	Ile Glu Ala.. ..tattccacagATA GAA GCA.. 3487
12	94	..Ser Glu G ..TCA GAA Ggtaagctgca.. 1246	3.0	lu Gly Pro.. ..ccttccacagAA GGC CCG.. 1253	30	53	..Tyr Phe Ar ..TAC TTC AGgtaaaactta.. 3532	1.0	g Gly Tyr.. ..attccctcagG GGC TAC.. 3540
13	110	..Ser Gln Lys ..TCT CAG AAGgtaagaccct.. 1364	0.9	Arg Glu Phe.. ..gtctcctcagCGG GAG TTC.. 1363	31	115	..Ala His Lys ..GCT CAC AAGgtaggtcaac.. 3646	2.9	Lys Ile Arg.. ..ctctgtgcagAAA ATC AGA.. 3655
14	185	..Leu Gly Ar ..CTG GGC CGgtgagtcatg.. 1540	0.6	g Arg Trp.. ..acggtgccagG CGC TGG.. 1548	32	66	..Ile Gly Gln ..ATT GGG CAGgtaggtgctg.. 3712	0.1	Ile Glu Gly.. ..ccccttttcagATC GAA GGT.. 3721
15	187	..Glu Ser Thr ..GAG TCC ACCgtaagtgcgt.. 1726	2.0	Asp Ser Gln.. ..gtgatcccagGAC AGC CAG.. 1735	33	189	..Ser Ser Lys ..TCG TCA AAGgtaagaaagt.. 3901	4.4	Gly Leu Gly.. ..tttcttgcagGGC CTC GGG.. 3910
16	93	..Thr Tyr Gln ..ACA TAC CAGgtcagtgagt.. 1828	1.4	Arg Val Asp.. ..tcctctctagAGA GTA GAT.. 1828	34	168	..Thr Asp Met ..ACG GAC ATGgtagggagct.. 4069	17.1	Ile Pro Arg.. ..ttttctttagATC CCG AGA.. 4078
17	170	..Arg Ile Il ..AGA ATC ATgtaaggaaat.. 1990	1.0	e Ser Ile ..ctgtgttcagA TCA ATC.. 1998	35	302	..Ile Ala Stop ..ATA GCT TAA 4153 ..GCAGCTGTCATTTCCTAAGAGgtAAGATCATTAAATTACAATGACAATGGCTCCAAGAGAGGGAAAAAGAGTTTTCAAACCATGTTCCATGGAACCCTGGA TTTATGCAAGCGTTCATTCAAATCGCTGTGCCTCAGCGCTAACAGGTTAATCTGCAGCACTAAAATGTCACAGCTTTGAATGATGATGACGCCAGTCAGAAGA TTATAGTCAACACTGAAGTTTTTATTTTAAATAAAATGAAAAATGAGAATGGAGTATATTAAGACATTTTAAACATTCTGTTCTCTGATTTGTGTGAGGTACT TACAACTTAAATGCAAAACTAAAGCCAAATCTGCTGATTTCTGCCTTTCTGGCTAGCTGGTGTTATCCAGAAGGGTGACCTATACTTGGGAGGTTCAGCCACT TCAATTTTGTGCTGTTGCCTTGATACAAAATTCAGAGCACTGAAGGTTTTGAAAAGTGACACTGGAATTCCCTGAATGAAATGTGTTGTCCACTTGGGAGGCA GAGGCAGGTGGATTTCTGAGTTCGAGGCCAGCCTGGTCTACAAAGTGAGTTCCAGGACAGTCAGGGCTACACAGAGAAACCCTGTCTCAAAAAAACAAAAAG AAAAAAAAAAA
18	115	..Val Asp Lys ..GTA GAT AAGgtatggatgg.. 2104	2.2	Val Leu Cys.. ..tactttacagGTT CTC TGT.. 2113	36	624	..ccttcctcagATATTTTAGTACCCAAGTGAAAAGCCAGCTTCTTACTCCTGACTGGACTGCATACTGTATTTGTACGCTGCTGGGCGGGAGGGAGGGGTGA GCCTTGTCACAAAATTTAGAATCACTATTCAAATCTAACCACATTAGAGAGATGAGGCATCTTACAAATTGTTTACTTAGGGTCCTCAGCTTAGAGGCCACCA GATAAGCACTGCAATGTTTGAAGCACTTTTAATGATTTGTCTTTGAAAACACTGAGTAAATGTTTGCTGCAGATGGAGGGAAAGGAAAGGAGACCTGGTGTGCA GACGCCATTTTTGCCTGAAAGAGCCTGCCAGCAACTATCATGATGCCTTTGACCAGGAGCCACTGAGCCTTAGCAGGGCGAGGTTTCTGCAAGGATTTTTTTC CTTTTTATCCCCCTCACCAGGAATAGGCTGTGGGTCTATGTATGTGTAGTTAACAGAAAAGAAGTGATATTTTCCTTGTGTTAGATGATTGTTCAGCAAGTGA ACATCCCTTTGGAATTTGAAGGGGAAAACAGTGTACAATTTTGAATGCATTATCACAAGATGTTTTTGTTTTTATTTGTATGGGGCTTTTTTTGTTTGCTTTT GTTTTGTTTGACTTTTTA

TABLE IV

Exon similarity of the rat and mouse Aox1, Aoh1, Aoh2, Aoh3, and Xor genes

The percentage of similarity between corresponding exons of the mouse and rat *Aox1, Aoh1, Aoh2, Aoh3,* and *Xor* genes was determined. The mean ± S.D. of the calculated similarities for each mouse/rat exon couple was determined and is shown. For each gene, the exons (hyperconserved) showing a percentage of similarity significantly above the 95th percentile of the distribution of all values are indicated along with the relative mouse/rat percentage similarity in parentheses. Similarly, exons (hyperdivergent) showing a percentage of similarity significantly below the 5th percentile are indicated along with the relative mouse/rat percentage similarity in parentheses. The statistical analysis was conducted according to the Shapiro-Wilk test using the SAS Version 8 software package.

	Exon similarity				
	Aox1 (93 ± 6)	*Aoh1* (90 ± 6)	*Aoh2* (89 ± 7)	*Aoh3* (95 ± 5)	*Xor* (94 ± 6)
			%		
Hyperconserved exons		1 (94)			
	2 (95)			2 (100)	2 (100)
	3 (97)				3 (100)
		4 (94)		4 (100)	
	5 (95)	5 (98)	5 (98)		5 (95)
	6 (95)		6 (100)	6 (100)	6 (100)
					7 (95)
		8 (96)	8 (96)	8 (96)	
				9 (100)	
				10 (100)	
	11 (94)		11 (92)	11 (96)	
	12 (100)	12 (91)			
			14 (95)		14 (97)
			15 (94)		15 (95)
			16 (90)		16 (100)
	17 (96)			17 (98)	17 (95)
		18 (92)		18 (100)	
			19 (95)		19 (98)
	20 (94)				
	21 (95)	21 (98)	21 (98)	21 (98)	21 (98)
	22 (96)	22 (96)		22 (96)	
	23 (96)	23 (93)	23 (93)	23 (96)	23 (100)
		24 (96)	24 (90)	24 (100)	
	25 (94)	25 (95)	25 (97)	25 (100)	25 (97)
					26 (96)
					27 (96)[a]
	27 (100)	27 (100)	27 (100)	27 (100)	28 (100)[a]
	28 (98)	28 (91)			
	29 (100)	29 (91)		29 (100)	
	30 (95)				31 (100)[a]
		31 (98)	31 (90)	31 (100)	32 (100)[a]
	32 (95)	32 (100)	32 (95)		33 (100)[a]
	33 (98)	33 (97)	33 (94)		34 (98)[a]
	34 (96)		34 (93)	34 (96)	35 (100)[a]
	35 (94)	35 (94)	35 (100)	35 (100)	
Hyperdivergent exons				1 (79)	1 (76)
	7 (77)	7 (74)	7 (66)		
			13 (72)		13 (77)
	16 (81)	16 (77)			

[a] Please note that exon 26 of *Xor* is split by an intron, which is not present in *Aox1*, *Aoh1*, *Aoh2*, and *Aoh3*. Hence, exons 27–36 of *xor* correspond to exons 26–35 of *Aox1*, *Aoh1*, *Aoh2*, and *Aoh3*.

AOH3 is endowed with a very selective pattern of tissue- and cell-specific localization in the mouse. In fact, although small amounts of the AOH3 transcript and possibly of the corresponding protein as well are detected in the skin, the richest and only other source of the enzyme is the olfactory mucosa. The modest amounts of AOH3 mRNA expressed in the skin hampered any attempt to define the specific cell population responsible for the synthesis of the transcript using *in situ* hybridization experiments. In this organ, it is possible that AOH3 co-localizes with the other molybdenum-containing aldehyde oxidase, AOH2, which is synthesized in the epidermal layer of the skin (14). Selective expression of mouse AOH3 in the olfactory mucosa is of remarkable interest, as aliphatic aldehydes are very strong odorants (54, 55). This suggests the possibility that AOH3 is involved in the perception of certain types of odorants in the mammalian organism. If this is the case, however, the enzyme must have an accessory role, as AOH3 is not present in the neuronal component of the olfactory epithelium, where the olfactory receptors are localized, and it is not synthesized in any of the other neuronal structures responsible for the transduction of the odorant stimuli. In contrast, our *in situ* hybridization experiments are compatible with a selective localization of AOH3 in the acinar and canalicular components of Bowman's glands that are localized in the subepithelial layer of the olfactory mucosa. Interestingly, a certain level of AOH3 mRNA expression is also evident in olfactory epithelial sustentacular cells, which are thought to have the same derivation as the epithelial cells of Bowman's glands (45). The selective localization of AOH3 in the nasal mucosa is compatible with a role of the enzyme in the production of some component of the mucous fluid. It is also possible that AOH3 is involved in the oxidation and inactivation of odorants and serves an accessory role in controlling the duration and/or strength of the olfactory stimulus that activates the olfactory receptors.

It is noticeable that the expression of the AOH3 transcript in the olfactory mucosa is highly reminiscent of that of CYP2A5, a member of the cytochrome P-450 family of monooxygenases (56). Like AOH3, CYP2A5 is localized in the glandular component of the nasal mucosa and in the sustentacular cells of the olfactory epithelium. The large family of CYP proteins is involved in the metabolism of numerous xenobiotics of pharmacological and toxicological importance, and the various CYP isoenzymes are believed to play an important protective role at

the level of the cells and tissues that synthesize them (57). This group of enzymes, showing broad substrate specificity, is localized in the endoplasmic reticulum of various cell types, including hepatocytes and pneumocytes. Co-localization of CYP2A5 and AOH3 in the same cells within the olfactory mucosa suggests that the two enzymes have similar functions or participate in the same metabolic pathway.

Toward a Definition of the Phylogeny of the Molybdo-flavoenzyme Genes—Molecular cloning of the cDNAs coding for mouse AOH3 and the rat orthologues of AOH3, AOH2, and AOH1 permitted the definition of the complete structure and organization of the corresponding genes. The mouse *Aoh3* gene shows remarkable conservation of the exon/intron organization relative to *Xor* and all members of the aldehyde oxidase gene cluster. Similarly, the exon/intron structure of rat *Aoh3*, *Aoh2*, and *Aoh1* is superimposable on that of *Aox1*, supporting the notion that all these genes originated from one or more duplication events. This last finding demonstrates that the existence of gene duplications coding for mammalian molybdo-flavoenzymes endowed with aldehyde oxidase activity is not a peculiarity of the mouse. The mouse *Aoh3* genes map to the same chromosomal region (chromosome 1 band c1) (15) and are transcribed in the same orientation as *Aox1*, *Aoh1*, and *Aoh2*. Analogously, a short section of rat chromosome 9q31 contains all the rat orthologues. In both animal species, the *Xor* gene orthologues reside on a different chromosome, chromosome 17 in mouse and chromosome 6 in rat. This is consistent with a more ancient origin of this last molybdo-flavoenzyme, which, unlike aldehyde oxidases, can be traced back to bacteria (1, 4, 5).

The rodent complement of molybdo-flavoenzymes is very similar to that of certain types of insects and plants (1). In fact, *Drosophila melanogaster* and *Arabidopsis thaliana* contain at least four forms of molybdo-flavoenzymes showing significant amino acid identity to AOX1, AOH1, AOH2, and AOH3. These proteins can be catalogued as aldehyde oxidases on the basis of various criteria (1). As in mice and rats, they are coded for by separate genes, whose structures suggest an origin common with the corresponding *Xor* gene through a series of duplication events (1). Despite these similarities, the duplications leading to the appearance of plant, insect, and rodent molybdo-flavoenzyme genes are distinct and must have taken place independently (1). In fact, the exon/intron structure of insect and plant aldehyde oxidase genes is much less complicated and quite different from that of mammalian aldehyde oxidase genes. This contrasts with the high level of amino acid identity among the five mammalian molybdo-flavoproteins and the perfect conservation of the exon/intron organization of the corresponding genes, suggesting that mouse and rat AOX1, AOH1, AOH2, and AOH3 arose relatively recently during evolution.

The recent release of the first draft of the dog and chicken genomes gives us an opportunity to take a look at the situation of the molybdo-flavoenzyme genes in two other higher vertebrates. The dog genome shows evidence of five potential genes coding for molybdo-flavoenzymes. All of these genes are characterized by remarkable sequence similarity to *Xor*, *Aox1*, *Aoh1*, *Aoh2*, and *Aoh3*. The first one maps to chromosome 17 and is characterized by sequence features that are consistent with the idea that the gene codes for the *Xor* orthologue (NCBI accession number AAEX01043817). The other four genes are localized very close to one another on chromosome 37 and present with the characteristics of the rat aldehyde oxidase genes (accession numbers AAEX01054799, AAEX01054803, AAEX01054804, and AAEX01054805). Strikingly, the exon/intron junctions of the five genes can be predicted precisely on the basis of the exon limits of the mouse and rat molybdo-flavoenzyme genes. This indicates that the duplication events giving rise to the whole complement of mammalian molybdo-flavoenzyme genes precede the divergence of carnivores from rodents during evolution. The situation of the chicken genome is rather different. In this animal species, there is evidence for the *Xor* orthologue and two extra genes coding for proteins characterized by high sequence similarity to AOX1, AOH1, AOH2, or AOH3. Once again, whereas *Xor* maps to chicken chromosome 3 (accession number AADN1028139), the other two loci map to chromosome 7 at a short distance from each other (accession numbers AADN01089740 and AADN01089742). This indicates that birds are already endowed with more than one aldehyde oxidase gene and that these genes cluster very close to each other, as observed in the case of mice, rats, and dogs. Reconstruction of the almost complete chicken *Xor* and two aldehyde oxidase homologues indicates structures and exon/intron organizations virtually identical to those of the rodent molybdo-flavoenzyme genes.[3] The three chicken molybdo-flavoenzymes are transcribed, as numerous ESTs corresponding to the products of each genetic locus are present in the data base. All this indicates that birds are endowed with a complement of functionally active molybdo-flavoenzyme genes that is smaller than that of rodents and carnivores. This finding suggests that the generation of the members of the mammalian molybdo-flavoprotein gene family was not synchronous and that a first round of gene duplication events took place during avian evolution.

The phylogeny of molybdo-flavoenzyme genes is probably more complicated than suggested by the simple scheme of successive gene duplication events depicted above. In fact, the complement of human and bovine molybdo-flavoenzyme proteins suggests gene inactivation events. Humans express the *Xor* gene, which is located on chromosome 2p, under the form of an active protein present in liver and milk (58–60). Furthermore, an aldehyde oxidase protein and the corresponding gene, named *Aox1* throughout the literature, have been reported (12, 16). As to other potential molybdo-flavoenzyme genes, although a portion of human chromosome 2q maintains three incomplete duplications of the *Aox1* gene, these duplications do not seem to code for functional proteins and are likely to represent transcribed, albeit inactive, pseudo-genes (1). A very similar situation may apply to bovines, although in this animal species, a reliable analysis of the molybdo-flavoenzyme complement can be based only on the evaluation of the EST data base. Indeed, searches for bovine sequences homologous to XOR, AOX1, AOH1, AOH2, or AOH3 invariably result in the identification of only two classes of incomplete cDNAs. The two classes correspond to ESTs coding for XOR and a single aldehyde oxidase protein, and this is similar to what is observed in humans.

In conclusion, these data suggest that the aldehyde oxidase duplicated genes present in rodents and birds must code for proteins that serve species-specific functions that are or that have become dispensable in certain types of mammals. In particular, rodents require multiple types of aldehyde oxidases for functions that are not shared or that may have been lost in humans and possibly bovines. Consistent with this idea, AOH3, the last addition to the molybdo-flavoenzyme family, is expressed solely in the olfactory organ, which is far more complex and developed in rodents and dogs than in humans. By the same token, AOH2 is present in large amounts in the papillae of the tongue, where it may serve a fundamental or an accessory function in the transduction of taste signals. Once again, the perception of taste is a specialized physiological function that is different in humans relative to other mammals. Further

[3] E. Garattini, unpublished data.

insight into the phylogeny of molybdo-flavoenzymes will be acquired as soon as the sequence data for other animal species (particularly primates) become available. A conclusive definition of the physiological function will likely require knockout animals for each aldehyde oxidase gene that we have already generated or that we are in the process of generating.

Acknowledgments—We thank Andrea Tedeschi and Ruth Vila for skillful assistance, Paolo Bigini for microphotographs, and Felice De Ceglie for excellent artwork. We are also thankful to Prof. Silvio Garattini for critical reading of the manuscript. We are particularly indebted to Dr. Frank Margolis (University of Maryland, Baltimore) for the useful discussion on the cellular localization of AOH3 within the olfactory mucosa.

REFERENCES

1. Garattini, E., Mendel, R., Romao, M. J., Wright, R., and Terao, M. (2003) *Biochem. J.* **372,** 15–32
2. Schindelin, H., Kisker, C., and Rajagopalan, K. V. (2001) *Adv. Protein Chem.* **58,** 47–94
3. Mendel, R. R., and Schwarz, G. (2002) *Metal Ions Biol. Syst.* **39,** 317–368
4. Ivanov, N. V., Hubalek, F., Trani, M., and Edmondson, D. E. (2003) *Eur. J. Biochem.* **270,** 4744–4754
5. Xiang, Q., and Edmondson, D. E. (1996) *Biochemistry* **35,** 5441–5450
6. Kappl, R., Huttermann, J., and Fetzner, S. (2002) *Metal Ions Biol. Syst.* **39,** 481–537
7. Xu, P., Hueckstead, T. P., Harrison, R., and Hoidal, J. R. (1994) *Biochem. Biophys. Res. Commun.* **199,** 998–1004
8. Saksela, M., and Raivio, K. O. (1996) *Biochem. J.* **315,** 235–239
9. Tsuchida, S., Yamada, R., Ikemoto, S., and Tagawa, M. (2001) *J. Vet. Med. Sci.* **63,** 353–355
10. Ichida, K., Amaya, Y., Noda, K., Minoshima, S., Hosoya, T., Sakai, O., Shimizu, N., and Nishino, T. (1993) *Gene* (*Amst.*) **133,** 279–284
11. Terao, M., Cazzaniga, G., Ghezzi, P., Bianchi, M., Falciani, F., Perani, P., and Garattini, E. (1992) *Biochem. J.* **283,** 863–870
12. Wright, R. M., Vaitaitis, G. M., Wilson, C. M., Repine, T. B., Terada, L. S., and Repine, J. E. (1993) *Proc. Natl. Acad. Sci. U. S. A.* **90,** 10690–10694
13. Calzi, M. L., Raviolo, C., Ghibaudi, E., de Gioia, L., Salmona, M., Cazzaniga, G., Kurosaki, M., Terao, M., and Garattini, E. (1995) *J. Biol. Chem.* **270,** 31037–31045
14. Terao, M., Kurosaki, M., Saltini, G., Demontis, S., Marini, M., Salmona, M., and Garattini, E. (2000) *J. Biol. Chem.* **275,** 30690–30700
15. Terao, M., Kurosaki, M., Marini, M., Vanoni, M. A., Saltini, G., Bonetto, V., Bastone, A., Federico, C., Saccone, S., Fanelli, R., Salmona, M., and Garattini, E. (2001) *J. Biol. Chem.* **276,** 46347–46363
16. Terao, M., Kurosaki, M., Demontis, S., Zanotta, S., and Garattini, E. (1998) *Biochem. J.* **332,** 383–393
17. Kurosaki, M., Demontis, S., Barzago, M. M., Garattini, E., and Terao, M. (1999) *Biochem. J.* **341,** 71–80
18. Cazzaniga, G., Terao, M., Lo Schiavo, P., Galbiati, F., Segalla, F., Seldin, M. F., and Garattini, E. (1994) *Genomics* **23,** 390–402
19. Wright, R. M., Clayton, D. A., Riley, M. G., McManaman, J. L., and Repine, J. E. (1999) *J. Biol. Chem.* **274,** 3878–3886
20. Berglund, L., Rasmussen, J. T., Andersen, M. D., Rasmussen, M. S., and Petersen, T. E. (1996) *J. Dairy Sci.* **79,** 198–204
21. Terao, M., Kurosaki, M., Zanotta, S., and Garattini, E. (1997) *Biochem. Soc. Trans.* **25,** 791–796
22. Harrison, R. (2002) *Free Radic. Biol. Med.* **33,** 774–797
23. Harrison, R. (2004) *Drug Metab. Rev.* **36,** 363–375
24. Vorbach, C., Scriven, A., and Capecchi, M. R. (2002) *Genes Dev.* **16,** 3223–3235
25. Ambroziak, W., Izaguirre, G., and Pietruszko, R. (1999) *J. Biol. Chem.* **274,** 33366–33373
26. Huang, D. Y., Furukawa, A., and Ichikawa, Y. (1999) *Arch. Biochem. Biophys.* **364,** 264–272
27. Tomita, S., Tsujita, M., and Ichikawa, Y. (1993) *FEBS Lett.* **336,** 272–274
28. Chambon, P. (1996) *FASEB J.* **10,** 940–954
29. Kastner, P., Mark, M., and Chambon, P. (1995) *Cell* **83,** 859–869
30. Lake, B. G., Ball, S. E., Kao, J., Renwick, A. B., Price, R. J., and Scatina, J. A. (2002) *Xenobiotica* **32,** 835–847
31. Rooseboom, M., Commandeur, J. N., and Vermeulen, N. P. (2004) *Pharmacol. Rev.* **56,** 53–102
32. Tatsumi, K., Kitamura, S., and Narai, N. (1986) *Cancer Res.* **46,** 1089–1093
33. Shaw, S., and Jayatilleke, E. (1990) *Biochem. J.* **268,** 579–583
34. Vila R., Kurosaki, M., Barzago, M. M., Kolek M., Bastone, A., Colombo L., Salmona, M., Terao, M., and Garattini, E. (2004) *J. Biol. Chem.* **279,** 8668–8683
35. Kozak, M. (1987) *Nucleic Acids Res.* **15,** 8125–8148
36. Sato, A., Nishino, T., Noda, K., Amaya, Y., and Nishino, T. (1995) *J. Biol. Chem.* **270,** 2818–2826
37. Nishino, T., and Nishino, T. (1997) *J. Biol. Chem.* **272,** 29859–29864
38. Nishino, T., and Nishino, T. (1989) *J. Biol. Chem.* **264,** 5468–5473
39. Enroth, C., Eger, B. T., Okamoto, K., Nishino, T., Nishino, T., and Pai, E. F. (2000) *Proc. Natl. Acad. Sci. U. S. A.* **97,** 10723–10728
40. Amaya, Y., Yamazaki, K., Sato, M., Noda, K., Nishino, T., and Nishino, T. (1990) *J. Biol. Chem.* **265,** 14170–14175
41. Holmes, R. S. (1979) *Biochem. Genet* **17,** 517–527
42. Ventura, S. M., and Dachtler, S. L. (1981) *Horm. Res.* (*Basel*) **14,** 250–259
43. Yoshihara, S., and Tatsumi, K. (1997) *Arch. Biochem. Biophys.* **338,** 29–34
44. Beedham, C., Critchley, D. J., and Rance, D. J. (1995) *Arch. Biochem. Biophys.* **319,** 481–490
45. Huard, J. M., Youngentob, S. L., Goldstein, B. J., Luskin, M. B., and Schwob, J. E. (1998) *J. Comp. Neurol.* **400,** 469–486
46. Demontis, S., Kurosaki, M., Saccone, S., Motta, S., Garattini, E., and Terao, M. (1999) *Biochim. Biophys. Acta* **1489,** 207–222
47. Rybczynski, R., Vogt, R. G., and Lerner, M. R. (1990) *J. Biol. Chem.* **265,** 19712–19715
48. Wittle, A. E., Kamdar, K. P., and Finnerty, V. (1999) *Mol. Gen. Genet.* **261,** 672–680
49. Mendel, R. R., and Hansch R. (2002) *J. Exp. Bot.* **53,** 1689–1698
50. Seo, M., Peeters, A. J., Koiwai, H., Oritani, T., Marion-Poll, A., Zeevaart, J. A., Koornneef, M., Kamiya, Y., and Koshiba, T. (2000) *Proc. Natl. Acad. Sci. U. S. A.* **97,** 12908–12913
51. Hoff, T., Frandsen, G. I., Rocher, A., and Mundy, J. (1998) *Biochim. Biophys. Acta* **1398,** 397–402
52. Godber, B., Sanders, S., Harrison, R., Eisenthal, R., and Bray, R. C. (1997) *Biochem. Soc. Trans.* **25,** 519S
53. Edmondson, D. E., and D'Ardenne, S. C. (1989) *Biochemistry* **28,** 5924–5930
54. Xu, F., Liu, N., Kida, I., Rothman, D. L., Hyder, F., and Shepherd, G. M. (2003) *Proc. Natl. Acad. Sci. U. S. A.* **100,** 13734–13735
55. Hatt, H., Gisselmann, G., and Wetzel, C. H. (1999) *Cell. Mol. Biol.* (*Noisy-Le-Grand*) **45,** 285–291
56. Piras, E., Franzen, A., Fernandez, E. L., Bergstrom, U., Raffalli-Mathieu, F., Lang, M., and Brittebo, E. B. (2003) *J. Histochem. Cytochem.* **51,** 1545–1555
57. Gonzalez, F. J., and Kimura, S. (2003) *Arch. Biochem. Biophys.* **409,** 153–158
58. Berger, R., Mezey, E., Clancy, K. P., Harta, G., Wright, R. M., Repine, J. E., Brown, R. H., Brownstein, M., and Patterson, D. (1995) *Somatic Cell Mol. Genet.* **21,** 121–131
59. Rytkonen, E. M., Halila, R., Laan, M., Saksela, M., Kallioniemi, O. P., Palotie, A., and Raivio, K. O. (1995) *Cytogenet. Cell Genet.* **68,** 61–63
60. Linder, N., Rapola, J., and Raivio, K. O. (1999) *Lab. Investig.* **79,** 967–974